Humidity-driven ABA depletion determines plant-pathogen competition for leaf water

Shigetaka Yasuda[1*], Akihisa Shinozawa[2,9], Yuanjie Weng[3,4,9], Arullthevan Rajendram[1,9], Taishi Hirase[1,9], Haruka Ishizaki[1], Ryuji Suzuki[5], Shioriko Ueda[1], Rahul Sk[6], Yumiko Takebayashi[3], Izumi Yotsui[2], Masatsugu Toyota[5,7,8], Masanori Okamoto[3], Yusuke Saijo[1*]

[1]Graduate School of Science and Technology, Nara Institute of Science and Technology, Ikoma, Japan. [2]Department of Bioscience, Tokyo University of Agriculture, Tokyo, Japan [3]Center for Sustainable Resource Science, RIKEN, Yokohama, Japan. [4]United Graduate School of Agricultural Science, Tokyo University of Agriculture and Technology, Fuchu, Japan. [5]Department of Biochemistry and Molecular Biology, Saitama University, Saitama, Japan. [6]The NODAI Genome Research Center (NGRC), Tokyo University of Agriculture, Tokyo, Japan. [7]Suntory Rising Stars Encouragement Program in Life Sciences (SunRiSE), Suntory Foundation for Life Sciences, Kyoto, Japan. [8]College of Plant Science and Technology, Huazhong Agricultural University, Wuhan, China. [9]These authors contributed equally: Akihisa Shinozawa, Yuanjie Weng, Arullthevan Rajendram, Taishi Hirase

*Corresponding authors: shige-yasuda@bs.naist.jp; saijo@bs.naist.jp

Abstract

Bacterial phytopathogens, such as *Pseudomonas syringae* pv. tomato (*Pst*) DC3000, induce water-soaked lesions in the leaf apoplast under high humidity, facilitating infection. However, it remains largely unclear how plants regulate their resistance to restrict bacterial infection in response to humidity. Here, we demonstrate that abscisic acid (ABA)-catabolizing ABA 8'-hydroxylase, encoded by *CYP707A3*, plays a critical role in this resistance in *Arabidopsis thaliana*. Elevated humidity induces *CYP707A3* expression, which is essential for reducing ABA levels and promoting stomatal opening, thereby limiting bacterial water-soaking and infection following leaf invasion. High humidity also increases cytosolic Ca^{2+} levels via the Ca^{2+} channels CNGC2 and CNGC4, with partial involvement from CNGC9, activating the calmodulin-binding transcription activator CAMTA3 to drive *CYP707A3* induction. However, *Pst* DC3000 counteracts this defense

response using type III secretion effectors, particularly AvrPtoB, facilitating water-soaking. These findings provide insights into the mechanisms underlying the competition between plants and bacteria for leaf water under elevated humidity.

Introduction

Bacterial phytopathogens cause foliar diseases that threaten plant survival and crop yields by proliferating within the leaf apoplast[1]. An important layer of defense against bacterial infection is provided by cell surface receptor-like kinases/proteins (RLKs/RLPs), collectively known as pattern recognition receptors (PRRs). PRRs detect microbe-associated molecular patterns (MAMPs) and endogenous damage-associated molecular patterns (DAMPs) to activate pattern-triggered immunity (PTI)[2-4]. Following ligand perception, PRRs form active complexes with co-receptors to trigger intracellular signaling cascades. This involves rapid cytosolic Ca^{2+} influx, a burst of reactive oxygen spices (ROS), activation of mitogen activated protein kinase (MAPK) cascades, production of defense-related phytohormones such as salicylic acid (SA), stomatal closure, transcriptional reprogramming, and production of antibacterial compounds[2-4]. To overcome PTI, bacterial pathogens deliver effector proteins into host tissues and cells via type III secretion (T3S) system[1]. The bacterial phytopathogen *Pseudomonas syringae* pv. *tomato* (*Pst*) DC3000 has 36 T3S effectors[5]. Recent studies have shown that *Pst* DC3000 utilizes specific effectors to manipulate the leaf apoplast environment, establishing conditions favorable for infection[6].

High humidity promotes foliar diseases caused by bacterial pathogens through multiple mechanisms. Initially, impaired stomatal closure facilitates bacterial invasion into leaves[7]. Once inside, bacterial pathogens induce apoplast hydration under high humidity, a critical process for disease development known as water-soaking[8]. To induce water-soaking, *Pst* DC3000 employs the highly conserved effectors HopM1 and AvrE, which manipulate the host plant's abscisic acid (ABA) pathways, a phytohormone critical for water retention[9,10]. Plants typically increase ABA levels under drought conditions to promote stomatal closure and conserve water[11]. However, under high humidity, when plants naturally reduce ABA levels, *Pst* DC3000 stimulates ABA biosynthesis and signaling in the host through HopM1 and AvrE, thereby enhancing water-soaking and promoting disease

progression[9,10]. Similarly, *Xanthomonas* bacteria exploit host ABA pathways through their effectors to facilitate leaf infection in rice, wheat, and Arabidopsis[12-14]. Despite recent advances in the identification and characterization of bacterial effectors involved in water-soaking, our understanding of the plant resistance mechanisms that counteract bacterial water acquisition remains limited[15,16].

In nature, high humidity often accompanies prolonged rainfall, inducing a wide range of physiological effects in plants, such as defects in cuticle formation, stomatal opening, changes in water uptake and transpiration, and leaf petiole movement (hyponasty)[7,17-19]. In Arabidopsis, high humidity rapidly induces transcriptional and post-transcriptional changes in leaves, modulating phytohormone pathways[17,19]. ABA levels are tightly regulated through the coordination of its biosynthesis and catabolism[20]. Under high humidity, ABA levels decrease via the action of *CYP707A1* and *CYP707A3*, which encode ABA 8'-hydroxylases, thereby facilitating stomatal opening[17]. Concurrently, the production and signaling of defense-promoting salicylic acid (SA) are suppressed, partly due to impaired ubiquitination of NPR1, an SA receptor and key transcriptional co-activator of SA-responsive genes, reducing its binding to target gene promoters[21]. Additionally, high humidity stimulates the biosynthesis of the gaseous phytohormone ethylene, which promotes leaf hyponasty[19]. Despite these extensive changes in phytohormone production and signaling, the mechanisms by which the modulation of host phytohormone pathways under high humidity impacts plant-pathogen interactions remain poorly understood.

In this study, we demonstrate that the high humidity-induced *CYP707A*3 plays a pivotal role in restricting bacterial water-soaking by promoting stomatal opening in leaves. High humidity elevates cytosolic Ca^{2+} concentrations via the Ca^{2+} channels CYCLIC NUCLEOTIDE-GATED CHANNEL 2 (CNGC2), CNGC4, and CNGC9, triggering *CYP707A3* induction through calmodulin-binding transcription activator 3 (CAMTA3). However, during infection, *Pst* DC3000 counteracts this signaling module and suppresses high humidity-induced transcriptional changes through its T3S effectors, with AvrPtoB playing a predominant role. These findings provide valuable insights into the mechanisms regulating plant-pathogen competition for leaf water under high humidity.

Result

CYP707A3 is required for resistance to bacterial water-soaking under high humidity

Upon exposure to high humidity, *CYP707A1* and *CYP707A3*, but not *CYP707A2* or *CYP707A4*, were transiently induced in wild-type (WT) leaves within 0.5 h (Fig. 1a). To investigate the role of *CYP707A1* and *CYP707A3* in bacterial resistance, we measured ABA levels and assessed bacterial water-soaking in the corresponding mutants. In WT plants, high humidity triggered a marked reduction in ABA levels within 2 h (Fig. 1b). This ABA decline was completely abolished in the *cyp707a1 cyp707a3* double mutant, which instead exhibited constitutively high ABA accumulation (Fig. 1b), indicating that these genes are required for humidity-induced ABA catabolism.

We next assessed water-soaking in *cyp707a* mutants (Supplementary Fig. 1a, b) using *Pst ΔhrcC*, a strain lacking a functional T3S system. Resistance to water-soaking was evaluated by monitoring leaf water retention following bacterial infiltration under high humidity. At 1 day post-inoculation (dpi), pronounced water-soaking was observed in *cyp707a3* and *cyp707a1 cyp707a3*, but not in WT, *cyp707a1*, or *cyp707a2* (Fig. 1c). The phenotype was more severe in *cyp707a1 cyp707a3* than in *cyp707a3*, suggesting a predominant role for *CYP707A3* with a partial contribution from *CYP707A1* in water-soaking resistance. Accordingly, we used *cyp707a1 cyp707a3* for most subsequent analyses. Under moderate humidity, however, even *cyp707a1 cyp707a3* displayed no detectable water-soaking (Fig. 1d). Consistently, *Pst* Δ*hrcC* growth was significantly higher in *cyp707a1 cyp707a3* than in WT under high humidity, but was indistinguishable under moderate humidity (Fig. 1e). These results demonstrate that *CYP707A3* is crucial for restricting water-soaking during *Pst* DC3000 infection, thereby limiting bacterial proliferation specifically under high humidity.

CYP707A3-mediated water-soaking resistance depends on stomatal opening

Pst DC3000 induces stomatal closure following leaf invasion to facilitate water-soaking[9,10]. Consistent with previous reports[17], loss of *CYP707A3* and *CYP707A1* impaired high-humidity-induced stomatal opening (Fig. 2a, b). To test whether

128 *CYP707A3*-mediated bacterial resistance is linked to stomatal regulation, we introduced
129 the *ost2-3D* mutation, an active allele of the plasma membrane H^+-ATPase AHA1 that
130 drives constitutive stomatal opening[22], into the *cyp707a1 cyp707a3* background
131 (Supplementary Fig. 2a, b). As expected, the *cyp707a1 cyp707a3 ost2-3D* triple mutant
132 exhibited enhanced stomatal opening compared with *cyp707a1 cyp707a*3 under both high
133 and moderate humidity (Fig. 2a, b). Correspondingly, water-soaking was almost
134 completely abolished in *cyp707a1 cyp707a3 ost2-3D* following *Pst ΔhrcC* infiltration,
135 similar to *ost2-3D* (Fig. 2c). This suppression was accompanied by markedly reduced *Pst*
136 Δ*hrcC* growth in both *cyp707a1 cyp707a3 ost2-3D* and *ost2-3D* (Fig. 2d). These findings
137 indicate that *CYP707A3* confers resistance to water-soaking, at least in part, by promoting
138 stomatal opening under high humidity.
139
140 **ABA depletion enhances bacterial resistance by restricting water-soaking**
141 **independently of SA under high humidity**
142 SA antagonizes many ABA-dependent processes and has been reported to suppress water-
143 soaking under light conditions[16,23,24]. However, both SA and ABA are required for
144 stomatal closure during early defense responses to bacterial phytopathogens[25]. To assess
145 whether SA influences *CYP707A3*-mediated water-soaking resistance, we introduced the
146 *sid2-2* mutation, which disrupts ICS1-dependent SA biosynthesis[26], into the *cyp707a1*
147 *cyp707a3* background (Supplementary Fig. 3a, b). The *cyp707a1 cyp707a3 sid2-2* triple
148 mutant, but not *sid2-2*, exhibited extensive water-soaking following *Pst* Δ*hrcC* infiltration
149 (Supplementary Fig. 3c), indicating that ICS1-dependent SA biosynthesis is dispensable
150 for *CYP707A3*-mediated water-soaking resistance.
151
152 We next tested whether ABA depletion alone is sufficient to confer bacterial resistance
153 under high humidity in an SA-independent manner. To this end, we examined water-
154 soaking and bacterial growth following *Pst* DC3000 infiltration in the *aao3* mutant, which
155 is deficient in ABA biosynthesis[27], with or without the *sid2-2* mutation (Supplementary
156 Fig. 3d, e). Consistent with previous studies on ABA dependence[9,10], *Pst* DC3000-
157 induced water-soaking was markedly reduced in *aao3*, irrespective of *sid2-2* mutation
158 (Supplementary Fig. 3f). This reduction correlated with decreased *Pst* DC3000 growth at
159 3 dpi in both *aao3* and *aao3 sid2*, although the effect was less pronounced in the latter

160 (Supplementary Fig. 3g). Under moderate humidity, however, suppression of *Pst* DC3000
161 growth by the *aao3* mutation was observed only in the presence of functional *SID2*
162 (Supplementary Fig. S3h), as reported previously[24]. Collectively, these results
163 demonstrate that ABA depletion confers resistance to *Pst* DC3000 under high humidity
164 by restricting water-soaking development, independently of the SA-ABA antagonism
165 observed under moderate humidity.
166
167 **CYP707A3/A1-mediated ABA depletion and PTI contribute additively to bacterial**
168 **resistance**
169 High humidity differentially affects PTI responses triggered by flg22, a MAMP derived
170 from bacterial flagellin[21]. To test whether high humidity-triggered ABA depletion via
171 *CYP707A3* and *CYP707A1* contributes to this modulation, we compared PTI marker gene
172 expression in WT and *cyp707a1 cyp707a3* following *Pst* Δ*hrcC* infiltration under
173 moderate and high humidity. After 24 h acclimation to the respective humidity conditions,
174 we measured *FRK1*, *NHL10*, and *PHI-1* expression at 1 h post-inoculation (hpi). Under
175 high humidity, *FRK1* induction was enhanced, *NHL10* induction was unchanged, and
176 *PHI-1* induction was abolished (Supplementary Fig. 4a). These patterns were similar in
177 WT and *cyp707a1 cyp707a3*, suggesting that CYP707A3/A1-mediated ABA depletion
178 has limited impact on the humidity-dependent PTI gene regulation.
179
180 We next examined the relationship between *CYP707A3*-mediated water-soaking
181 resistance and PTI by crossing *cyp707a1 cyp707a3* with the *bak1-5 bkk1 cerk1* triple
182 mutant (hereafter *bbc*), which disrupts PRR activation mediated by the co-receptors
183 BAK1, BKK1, and CERK1[28] (Supplementary Fig. 4b, c). The *cyp707a1 cyp707a3 bbc*
184 quintuple mutant exhibited pronounced water-soaking following *Pst* Δ*hrcC* infiltration,
185 similar to *cyp707a1 cyp707a3* (Supplementary Fig. 4d). By contrast, *bbc* showed WT-
186 like or slightly enhanced resistance to water-soaking (Supplementary Fig. 4d), indicating
187 that humidity-triggered ABA depletion restricts water-soaking independently of
188 BAK1/BKK1/CERK1-dependent PTI branches. Notably, *Pst* Δ*hrcC* growth was
189 significantly higher in *cyp707a1 cyp707a3 bbc* compared to either *cyp707a1 cyp707a3*
190 or *bbc* (Supplementary Fig. 4e), indicating additive effects. Together, these results
191 indicate that CYP707A3/A1-mediated ABA depletion and BAK1/BKK1/CERK1-

192 dependent PTI pathways contribute additively to *Pst* DC3000 resistance under high
193 humidity.
194
195 **Global transcriptome analysis reveals CAMTA binding motif enrichment in early-**
196 **phase high humidity-induced genes**
197 To capture transcriptional reprogramming triggered by high humidity, we performed
198 RNA-sequencing (RNA-seq) on WT leaves exposed to moderate or high humidity for 0.5
199 and 5 h. In total, 2394 up-regulated and 2054 down-regulated genes were identified as
200 differentially expressed (DEGs: fold change > 2, FDR < 0.05) under high humidity
201 compared with moderate humidity (Fig. 3a and Supplementary Table 1). The DEGs
202 identified at 0.5 h and 5 h showed limited overlap (up-regulated: 43.5% of 0.5 h and
203 30.5% of 5 h; down-regulated: 30% of 0.5 h and 6.7% of 5 h) (Fig. 3a), suggesting that
204 distinct regulatory mechanisms are involved during early and late stages of the response.
205 This distinction was further supported by principal component analysis (PCA), which
206 revealed clear separation of transcriptomes according to both humidity conditions and
207 exposure durations (Fig. 3b).
208
209 K-means clustering of the 1000 most variable genes yielded 10 distinct clusters (Fig. 3c
210 and Supplementary Table 2). High humidity-induced genes were distributed across four
211 clusters, with *CYP707A1* and *CYP707A3* notably present in Cluster 6 (Fig. 3c). Clusters
212 2 and 6 exhibited rapid transcriptional upregulation within 0.5 h of treatment, Cluster 9
213 peaked at 0.5 h and gradually declined by 5 h while remaining elevated under high
214 humidity relative to moderate humidity, and Cluster 1 was primarily induced at 5 h (Fig.
215 3c). Gene ontology analysis highlighted over-represented biological processes in these
216 clusters, including 'hypoxia response' (Clusters 1 and 2), 'jasmonate (JA) response'
217 (Cluster 6), and 'cell wall biogenesis' (Cluster 9) (Supplementary Fig. 5). Notably, *Cis*-
218 regulatory motif analysis revealed significant enrichment of CAMTA binding motifs,
219 particularly in Clusters 2 and 6 (Fig. 3d), implicating CAMTA transcription factors as
220 potential key regulators of early transcriptional responses to high humidity.
221
222 **High humidity-induced *CYP707A3* expression requires CAMTA binding motifs in**
223 **its promoter**

224 The promoter region of *CYP707A3* contains two tandem CAMTA binding motifs (CGCG-
225 box), whereas the *CYP707A1* promoter lacks these elements (Fig. 4a). To assess the
226 contribution of these motifs to high humidity-induced *CYP707A3* expression, we
227 transiently expressed a GUS reporter driven by either a native *CYP707A3* promoter
228 (harboring both CGCG-boxes) or a modified promoter lacking these motifs (ΔCGCG) in
229 *NahG* plants (Supplementary Fig. 6a), which are depleted of SA to facilitate
230 Agrobacterium-mediated gene delivery. *GUS* expression driven by the native promoter
231 was significantly induced 0.5 h after high humidity exposure, whereas the ΔCGCG
232 promoter failed to confer this induction (Fig. 4b). In these plants, high humidity induction
233 of endogenous *CYP707A3* expression remained unaffected (Fig. 4b). These results
234 indicate that CAMTA binding motifs mediate, at least in part, the high humidity
235 responsiveness of the *CYP707A3* promoter.
236
237 To evaluate the physiological relevance of this regulation, we generated *cyp707a3*
238 transgenic plants expressing CYP707A3 fused to a C-terminal 3×FLAG tag (CYP707A3-
239 FLAG), driven by either the native or ΔCGCG promoter (Supplementary Fig. 6b, c).
240 Consistent with the GUS reporter results, high humidity-induced *CYP707A3-FLAG*
241 expression was markedly reduced in the ΔCGCG promoter line compared with the native
242 promoter line (Supplementary Fig. 6d). Following *Pst* Δ*hrcC* infiltration, the impaired
243 water-soaking resistance of *cyp707a3* was fully restored by *CYP707A3-FLAG* expressed
244 under the native promoter, but only partially restored under the ΔCGCG promoter
245 (Supplementary Fig. 6e). Together, these findings indicate that CAMTA-binding motifs
246 in the *CYP707A3* promoter are critical for its high humidity-induced expression and for
247 conferring resistance to bacterial water-soaking.
248
249 **High humidity triggers intracellular Ca^{2+} signaling to induce *CYP707A3* expression**
250 CAMTA transcription factors are activated upon binding to Ca^{2+}-CaM[29]. Given their
251 putative role in high humidity-induced transcription, we hypothesized that elevated
252 humidity triggers an increase in cytosolic Ca^{2+} levels. Using *35S::GCaMP3* plants
253 expressing the Ca^{2+} biosensor GCaMP3, we detected a rapid rise in cytosolic Ca^{2+} in leaf
254 cells within 10 min of high humidity exposure (Supplementary Fig. 7a, b and
255 Supplementary Movie 1). To test whether cytosolic Ca^{2+} influx contributes to high

256 humidity-induced *CYP707A3* and *CYP707A1* expression, we applied the Ca^{2+} channel
257 inhibitors $LaCl_3$ and $GdCl_3$ prior to humidity treatment. Both inhibitors significantly
258 suppressed *CYP707A3* induction, but did not suppress *CYP707A1* (Supplementary Fig.
259 7c), indicating a specific requirement for Ca^{2+} signaling in *CYP707A3* induction.
260 Temporal expression profiling further revealed that high humidity-triggered cytosolic
261 Ca^{2+} elevation precedes *CYP707A3* induction (Supplementary Fig. 7b, d). These findings
262 indicate that humidity elevation triggers cytosolic Ca^{2+} influx in leaves, which in turn
263 mediates *CYP707A3* expression.
264
265 **CNGC2/4/9 play a critical role in high humidity-induced *CYP707A3* expression**
266 CNGCs, comprising 20 members in Arabidopsis, mediate cytosolic Ca^{2+} influx in diverse
267 physiological processes[30]. To assess their role in high humidity-triggered Ca^{2+} signaling,
268 we examined *CYP707A3* induction in loss-of-function mutants of individual *CNGCs*. An
269 initial screen in 2-week-old plants revealed that high humidity-induced *CYP707A3*
270 expression was significantly reduced in *cngc2*, *cngc4*, and *cngc9* (Supplementary Fig. 8a,
271 b). Subsequent analysis in 5-week-old plants showed that high humidity induction of both
272 *CYP70A3* and *CYP707A1* was impaired in *cngc2* and *cngc4*, whereas only *CYP707A3*
273 induction was reduced in *cngc9* (Fig. 4c). These results suggest that CNGC2 and CNGC4
274 act cooperatively to mediate Ca^{2+} influx required for high humidity-induced *CYP707A3*
275 expression, with partial contribution from CNGC9. Collectively, these findings suggest
276 that CNGC2/4-mediated cytosolic Ca^{2+} elevation, together with partial support from
277 CNGC9, is crucial for *CYP707A3* and *CYP707A1* induction in response to high humidity.
278
279 **CAMTA3 drives *CYP707A3* induction, ABA depletion, and resistance to bacterial**
280 **water-soaking under high humidity**
281 Among the six CAMTA transcription factors in Arabidopsis, CAMTA3 is a central
282 regulator of responses to diverse stimuli[31-34]. To assess its role in high humidity-induced
283 *CYP707A3* expression, we used an inactive CAMTA3-A855V variant, which carries
284 A855V substitution in the IQ domain that disrupts CAMTA3 function without triggering
285 SA defense activation[35]. Introduction of *CAMTA3* or *CAMTA3-A855V* under the control
286 of a native *CAMTA3* promoter in the *camta2 camta3* mutant background did not alter
287 plant growth or basal SA levels (Supplementary Fig. 9a-c). *CAMTA3* expression restored

288 WT-like responses to high humidity, including *CYP707A3* induction, ABA depletion, and
289 stomatal opening (Fig. 4d-f). In contrast, these responses were markedly impaired in
290 *CAMTA3-A855V*-expressing plants (Fig. 4d-f), indicating that CAMTA3 activity is
291 required for their induction. Consistent with the absence of CGCG motifs in the
292 *CYP707A1* promoter, high humidity-induced *CYP707A1* expression was unaffected in
293 either *CAMTA3*- or *CAMTA3-A855V*-expressing plants (Fig. 4d), underscoring distinct
294 regulatory mechanisms for *CYP707A3* and *CYP707A1* expression. Moreover, the levels
295 of SA and jasmonoyl-isoleucine (JA-Ile), the major bioactive form of JA, remained
296 unchanged across plant genotypes and humidity treatments (Supplementary Fig. 9c).
297 Together, these findings indicate that CAMTA3 promotes ABA depletion and stomatal
298 opening under high humidity by inducing *CYP707A3*, without altering SA or JA
299 accumulation.
300
301 We next tested whether CAMTA3 activity is required to suppress bacterial water-soaking
302 and proliferation under high humidity. Plants expressing *CAMTA3-A855V*, but not
303 *CAMTA3*, exhibited extensive water-soaking and permitted increased growth of *Pst* Δ*hrc*
304 under high humidity (Fig. 4g, h), whereas bacterial growth was unaffected under
305 moderate humidity (Fig. 4i). These findings demonstrate that CAMTA3 activity is
306 required for resistance to bacterial water-soaking and infection specifically under high
307 humidity. This is consistent with a model in which elevated humidity triggers Ca^{2+} influx
308 through CNGC2/4/9, activating CAMTA3 to drive *CYP707A3*-mediated resistance.
309
310 **_Pst_ DC3000 suppresses high humidity-induced _CYP707A3_ expression via type III**
311 **secretion effectors**
312 *Pst* DC3000 enhances host ABA responses by manipulating ABA biosynthesis, signaling,
313 and translocation to promote water-soaking under high humidity[9,10]. We tested whether
314 *Pst* DC3000 also targets high humidity-triggered ABA depletion via *CYP707A3* and
315 *CYP707A1*. WT leaves were inoculated with *Pst* DC3000, *Pst* Δ*hrcC*, and *Pst* Δ28E
316 (lacking 28 T3S effectors)[36]. At 8 hpi under moderate humidity, plants were shifted to
317 moderate or high humidity for 0.5 h before RT-qPCR analysis (Fig. 5a). At this point,
318 bacterial populations were comparable between *Pst* DC3000 and *Pst* Δ*hrcC* (Fig. 5b),
319 minimizing potential effects of differential bacterial growth. Under these conditions,

320 *CYP707A1* was not induced by high humidity, even in the absence of bacterial inoculation
321 (Fig. 5C), likely due to desensitization from water infiltration. By contrast, *CYP707A3*
322 was significantly induced by high humidity in mock-inoculated leaves and in those
323 inoculated with *Pst* Δ*hrcC* or *Pst* Δ28E, but this induction was markedly suppressed by
324 *Pst* DC3000 (Fig. 5c). CAMTA3 protein accumulation was unaffected by inoculation
325 with the WT or mutant bacteria (Supplementary Fig. 10), suggesting that suppression is
326 not due to CAMTA3 depletion. Consistent with previous reports[9,10], *Pst* DC3000, but not
327 *Pst* Δ*hrcC* or *Pst* Δ28E, also induced *NCED3*, encoding a key ABA biosynthesis enzyme,
328 under these conditions (Fig. 5c). Together, these results indicate that *Pst* DC3000 employs
329 T3S effectors to suppress *CYP707A3* induction while promoting *NCED3* expression,
330 thereby maintaining elevated ABA levels under high humidity to facilitate infection.
331
332 ***Pst* DC3000 blocks high humidity-driven plant transcriptome reprogramming via**
333 **type III secretion effectors**
334 To further investigate how *Pst* DC3000 modulates plant responses to high humidity, we
335 performed RNA-seq analysis on leaves inoculated with *Pst* DC3000, *Pst* Δ*hrcC*, and *Pst*
336 Δ28E for 8 h, followed by a 0.5 h of exposure to moderate or high humidity. PCA revealed
337 a clear separation of leaf transcriptomes based on humidity conditions in non-inoculated
338 leaves and those inoculated with *Pst* Δ*hrcC* or *Pst* Δ28E (Fig. 5d). In contrast, this
339 separation was absent in leaves inoculated with *Pst* DC3000 (Fig. 5d), indicating that *Pst*
340 DC3000 broadly disrupts transcriptomic responses to high humidity via T3S effectors. K-
341 means clustering of the 2000 most variable genes resulted in 10 distinct clusters (Fig. 5e
342 and Supplementary Table 3). High humidity-induced genes were enriched in three
343 clusters, with Clusters 3 and 8 containing *CYP707A1* and *CYP707A3*, respectively (Fig.
344 5e). *Pst* DC3000 strongly suppressed high humidity-induced up-regulation in Clusters 3
345 and 8, and partially in Cluster 4 (Fig. 5e). Notably, Cluster 3 genes were upregulated
346 following *Pst* DC3000 inoculation under moderate humidity, irrespective of subsequent
347 humidity conditions (Fig. 5e). These findings indicate that *Pst* DC3000, through T3S
348 effectors, not only suppresses CAMTA3-regulated genes but also broadly alters early
349 transcriptional networks responsive to high humidity during infection.
350
351 **AvrPtoB contributes to suppression of *CYP707A3*-mediated water-soaking**

352 **resistance**

353 To identify the bacterial effector(s) responsible for suppressing *CYP707A3* induction
354 under high humidity, we analyzed multiple effector-deletion mutants of *Pst* DC3000[36].
355 High humidity-induced *CYP707A3* expression was significantly suppressed in WT leaves
356 at 8 hpi with *Pst* Δ14E (lacking 14 T3S effectors) and *Pst* Δ20E (lacking 20 T3S effectors),
357 similar to *Pst* DC3000 (Fig. 6a), at a time when T3S-dependent bacterial growth was not
358 evident (Fig. 5b). In contrast, *Pst* Δ28E failed to suppress *CYP707A3* induction,
359 indicating that one or more of the remaining eight effectors (*HopK1*, *HopY1*, *HopB1*,
360 *HopAF1*, *AvrPtoB*, *AvrPto*, *HopE1*, and *HopA1*) are required for this suppression (Fig.
361 6a).

362

363 Given that *in-planta* expression of *AvrPtoB* has been associated with increased ABA
364 levels through induction of *NCED3*[37], we tested whether AvrPtoB contributes to
365 *CYP707A3* suppression. To this end, we generated transgenic plants expressing either
366 *AvrPtoB* or its partially redundant counterpart, *AvrPto*[38], under a DEX-inducible promoter
367 (*DEX::AvrPtoB* and *DEX::AvrPto*; Fig. 6b, c and Supplementary Fig. 11a). Following
368 DEX treatment, high humidity-induced *CYP707A3* expression was specifically
369 suppressed in *DEX::AvrPtoB*, but not in *DEX::AvrPto*, despite lower protein
370 accumulation of AvrPtoB compared to AvrPto (Fig. 6b, c and Supplementary Fig. 11b).
371 An E3 ubiquitin ligase-deficient variant, AvrPtoB-F479A[39], retained the ability to
372 suppress *CYP707A3* induction (Fig. 6d and Supplementary Fig. 11a), suggesting that this
373 activity is independent of its E3 ligase function. In contrast, high humidity induction of
374 *CYP707A1* was specifically suppressed in *AvrPto*-expressing leaves (Supplementary Fig.
375 11c-e). Collectively, these findings suggest that bacteria selectively target *CYP707A3* and
376 *CYP707A1* with distinct T3S effectors, AvrPtoB and AvrPto, respectively, under high
377 humidity.

378

379 Consistent with the predominant role for *CYP707A3* in water-soaking resistance (Fig. 1c),
380 high humidity-triggered ABA depletion and stomatal opening were also compromised in
381 *DEX::AvrPtoB* following DEX treatment (Fig. 6e, f). Importantly, DEX-induced *AvrPtoB*
382 expression substantially restored water-soaking in leaves infiltrated with *Pst* DC3000
383 *ΔhrcC* (Fig. 6g). The results indicate that AvrPtoB plays a critical role in counteracting

384 *CYP707A3*-mediated water-soaking resistance under high humidity.

385

386 ***Pst* DC3000 employs AvrPtoB to suppress *CYP707A3* expression and promote water-**
387 **soaking under high humidity**

388 We next evaluated the physiological relevance of AvrPtoB and AvrPto in promoting ABA-
389 dependent bacterial infection under high humidity using *Pst* DC3000 mutant strain
390 lacking both *AvrPtoB* and *AvrPto* (*Pst* Δ*avrPtoB* Δ*avrPto*). Plants were shifted from
391 moderate to high humidity at 2 hpi, following conditions conventionally used in previous
392 studies[8-10] (Fig. 7a and Supplementary Fig. S12a). RT-qPCR analysis revealed that
393 *CYP707A3* expression was suppressed from 6 to 24 hpi with *Pst* DC3000, despite
394 continuous high humidity from 2 hpi (Supplementary Fig. S12b). This suppression was
395 absent with *Pst* Δ28E, whereas with *Pst* Δ*avrPtoB* Δ*avrPto* it was impaired at 6 hpi
396 but restored at 12-24 hpi (Supplementary Fig. S12b), indicating that AvrPtoB and/or
397 AvrPto mediate early suppression of *CYP707A3*, while other effectors contribute to later
398 suppression. Consistently, ABA levels increased at 6 hpi with *Pst* DC3000, but not with
399 *Pst* Δ*avrPtoB* Δ*avrPto* or *Pst* Δ28E (Supplementary Fig S12c). This initial increase was
400 followed by further accumulation at 12 and 24 hpi with *Pst* DC3000 and partially with
401 *Pst* Δ*avrPtoB* Δ*avrPto*, but not with *Pst* Δ28E. Together, these findings indicate that
402 AvrPtoB- and/or AvrPto-mediated suppression of *CYP707A3* is essential for the initial
403 phase of ABA accumulation under high humidity, which is critical for subsequent water-
404 soaking and bacterial proliferation.

405

406 To dissect individual contributions of these effectors, we generated *Pst* DC3000 mutant
407 strains lacking either *AvrPtoB* (*Pst* Δ*avrPtoB*) or *AvrPto* (*Pst* Δ*avrPto*) (Fig. 7b and
408 Supplementary Fig. S13a, b). The two effectors did not affect each other's expression
409 during infection (Fig. 7b). Consistent with DEX induction (Fig. 6b, c), high humidity-
410 induced *CYP707A3* expression was suppressed by *Pst* DC3000 and *Pst* Δ*avrPto*, but
411 permitted with *Pst* Δ*avrPtoB* and *Pst* Δ*avrPtoB* Δ*avrPto* (Fig. 7b). By contrast, enhanced
412 *CYP707A1* expression relative to *Pst* DC3000 was observed only with *Pst* Δ*avrPtoB*
413 Δ*avrPto* (Fig. 7b), suggesting redundancy in *CYP707A1* suppression. For *NCED3*

414 induction, *Pst* Δ*avrPto* resembled *Pst* DC3000, whereas *Pst* Δ*avrPtoB* and *Pst* Δ*avrPtoB*
415 Δ*avrPto* failed to induce it (Fig. 7b), indicating a predominant role of AvrPtoB in both
416 *CYP707A3* suppression and *NCED3* induction. Correspondingly, ABA accumulation at 6
417 hpi was enhanced with *Pst* DC3000 and *Pst* Δ*avrPto*, but not with *Pst* Δ*avrPtoB* or *Pst*
418 Δ*avrPtoB* Δ*avrPto* (Fig. 7c). Together, these results indicate that AvrPtoB is the primary
419 determinant of ABA accumulation under high humidity, acting through both *CYP707A3*
420 suppression and *NCED3* induction.
421
422 We next assessed the impact of AvrPtoB on bacterial water-soaking and infection. Under
423 high humidity, *Pst* DC3000 induced extensive water-soaking, which was strongly reduced
424 in leaves infiltrated with *Pst ΔavrPtoB* or *Pst ΔavrPtoB ΔavrPto*, while *Pst ΔavrPto*
425 retained partial activity (Supplementary Fig. 13c, d). These results indicate a predominant
426 role for AvrPtoB, with a moderate contribution from AvrPto. Importantly, delayed
427 suppression of *CYP707A3* by *Pst* Δ*avrPtoB* Δ*avrPto* at 12-24 hpi (Supplementary Fig.
428 12b) was insufficient to promote water-soaking, highlighting the importance of early
429 ABA depletion for this virulence activity. Moreover, *Pst* Δ*avrPtoB* induced smaller water-
430 soaked area compared to *Pst* DC3000 even in *cyp707a1 cyp707a3* leaves (Fig, 7d, e).
431 This reduction correlated with milder disease symptoms and lower bacterial growth in
432 both WT and *cyp707a1 cyp707a3* plants (Fig. 7f, g). These findings indicate that AvrPtoB
433 also targets an additional, *CYP707A1*/*CYP707A3*-independent layer of water-soaking
434 resistance, which may align with the additive roles of BAK1/BKK1/CERK1-mediated
435 PTI and ABA-catabolism-mediated defenses in restricting bacterial growth under high
436 humidity (Supplementary Fig. 4d, e).
437
438 **Discussion**
439 Terrestrial plants are constantly exposed to fluctuations in air humidity and have evolved
440 elaborate adaptation mechanisms[17,19,40-42]. High humidity, often following prolonged
441 rainfall, substantially exacerbates plant diseases caused by fungal and bacterial
442 pathogens[8,43]. It is therefore plausible that plants pre-condition or activate defense
443 responses in anticipation of these threats when sensing increased humidity. In this study,
444 we demonstrate that the CNGC2/4/9-CAMTA3-CYP707A3 module is involved in
445 response to elevated humidity, conferring bacterial resistance (Fig. 7h). Our findings

446 suggest that high humidity acts as a danger signal to enhance defense readiness. This
447 aligns with earlier studies that high humidity induces ROS accumulation in Arabidopsis
448 leaf apoplast, a hallmark of defense responses during pathogen challenge[19,21].
449 Additionally, high humidity increases cuticle permeability, which has been associated
450 with enhanced resistance to the fungal pathogen *Botrytis cinerea*[18,44,45]. Rainfall and
451 submergence have also been linked to strengthened disease resistance in plants[34,46]. These
452 findings suggest that plants possess the mechanisms linking the sensing of increased
453 water or humidity levels to the activation or reinforcement of defense responses. Our
454 findings reveal a mechanism linking humidity perception to the activation of defenses
455 that prevent bacterial access to leaf water.
456
457 Antagonistic interactions between ABA and SA signaling have been well
458 documented[23,24,47,48], yet their modulation under varying environmental conditions
459 remain under-explored. In Arabidopsis, *CYP707A3* overexpression enhances
460 transpiration rates[49]. ABA application suppresses systemic acquired resistance (SAR)
461 inducers acting both upstream and downstream of SA accumulation[23]. Enhanced SA
462 production under continuous light suppresses *Pst* DC3000-induced water-soaking
463 without interfering with *NCED3* induction[16]. We show that CYP707A3-mediated ABA
464 depletion confers water-soaking resistance independently of SA under high humidity,
465 whereas ABA deficiency enhances bacterial resistance in an SA-dependent manner under
466 moderate humidity. These observations underscore a humidity-dependent differentiation
467 in bacterial virulence strategies and the role of ABA depletion in bacterial resistance. The
468 distinct regulation of SA-ABA antagonism aligns with the decrease in SA production and
469 effectiveness under high humidity[21]. Notably, however, genes associated with SA defense,
470 such as *SARD1*, *CBP60g*, and *BCS1*[50-52], are induced under high humidity even in the
471 absence of pathogen challenge (Cluster 3 in Fig 5e and Supplementary Table 3),
472 suggesting potential coupling between humidity sensing and SA-mediated resistance,
473 which may be further potentiated by PRR signaling (Supplementary Fig. 4e).
474
475 To our knowledge, this study provides the first evidence that phytopathogens promote
476 infection by suppressing high humidity responses in host plants through effector proteins.
477 Our RNA-seq analyses (Fig. 5d, e) demonstrate that *Pst* DC3000 employs multiple T3S

effectors to inhibit humidity-triggered transcriptomic changes, thereby circumventing *CYP707A3*-mediated water-soaking resistance (Fig. 7h). Interestingly, *Pst* DC3000 T3S effectors also induce a subset of humidity-inducible genes, including *CYP707A1*, regardless of humidity conditions (Fig. 5e). The functional significance of their induction represents an open question for future studies. *CYP707A1* is predominantly induced in guard cells under high humidity[17] and *Pst* DC3000 elevates ABA levels in guard cells[10]. Whether bacterial *CYP707A1* induction occurs specifically in guard cells or in other tissues remains to be determined. Suppression of *CYP707A3* induction alone is sufficient to permit ABA-mediated stomatal closure, facilitating water-soaking under high humidity, as indicated by the impaired water-soaking resistance in *cyp707a3* mutants (Fig. 1c). Recent findings indicate that post-invasion stomatal reopening, rather than the initial closure to restrict bacterial entry, is critical for resisting bacterial water-soaking and infection[53], emphasizing the role of CYP707A-mediated ABA depletion as a core defense barrier limiting bacterial access to apoplastic water.

We identify AvrPtoB as a major T3S effector suppressing this defense. Genetic analyses show that among the 36 T3S effectors, AvrPtoB has a prominent role in blocking high humidity-induced *CYP707A3* expression (Fig. 7h). Earlier studies reported that AvrPtoB can target CYP707A3 and paralogs for proteasomal degradation when these proteins are transiently expressed in *Nicotiana benthamiana*[54]. By suppressing ABA catabolism and simultaneously promoting ABA biosynthesis via *NCED3* induction[37,54], AvrPtoB manipulates both arms of host ABA balance, facilitating stomatal closure and maintaining elevated ABA under high humidity. How AvrPtoB E3 ubiquitin ligase activity, known to act on membrane-localized immune receptors and transcription cofactors[55-60], contributes to suppression of *CYP707A3* and induction of *NCED3* remains to be determined.

Our work identifies CAMTA3 transcription regulator and CNGC2/4/9 Ca^{2+} channels as key regulators of humidity-induced *CYP707A3* expression, consistent with recent findings[61]. While the oomycete effector AVRblb2 has been shown to suppress CNGC activity[62], the potential targeting of CNGCs by *Pst* DC3000 effectors remains unexplored. Notably, the presence of a dominant-negative CAMTA3-A855V allele significantly impairs resistance to bacterial and fungal pathogens, SAR, as well as early transcriptional

510 responses shared by PTI, effector-triggered immunity and abiotic stress responses[63-65].
511 This underscores the critical role of CAMTA3 in promoting and/or priming defense
512 activation under high humidity. The disruption of *CAMTA1/2/3* is also linked to
513 nucleotide-biding leucine-rich repeat receptor activation leading to SA defense activation
514 and autoimmunity[35,66], suggesting that CAMTAs might be targeted by pathogen effectors
515 to counteract humidity-induced defenses. Future studies on AvrPtoB and other effectors,
516 including HopAM1, HopM1, and AvrE, which promote ABA responses[9,42,67], and their
517 interactions with the CNGC2/4/9-CAMTA3-CYP707A3 signaling module and another
518 water-soaking defense(s) will deepen our understanding of the interplay between
519 humidity-triggered defenses and effector-mediated host manipulation. This work
520 advances our knowledge of how plants and pathogens optimize immunity and virulence
521 strategies under high humidity, driven by their competition for water as a decisive factor.
522
523 **Methods**
524
525 **Plant materials and growth conditions**
526 Arabidopsis accession Columbia-0 (Col-0) was used as the wild-type (WT) in this study.
527 The *cyp707a1 cyp707a3 ost2-3D*, *cyp707a1 cyp707a3 sid2-2*, *aao3 sid2-2*, *bak1-5 bkk1*
528 *cerk1* (*bbc*), and *cyp707a1 cyp707a3 bbc* mutants were generated by genetic crossing.
529 The genotypes of Arabidopsis mutants and transgenic lines were verified by PCR, Sanger-
530 sequencing, or chemical selection. Plant materials and genotyping primers used are listed
531 in Supplementary Tables 4 and 6, respectively.
532
533 Surface-sterilized seeds were sown on half-strength Murashige and Skoog (MS) medium
534 [2.3 g/L Murashige and Skoog Plant Salt Mixture (FUJIFILM Wako Pure Chemical, Cat#
535 392-00591), 1% (w/v) sucrose, 0.5 g/L MES, 1% (w/v) agar (FUJIFILM Wako Pure
536 Chemical, Cat# 016-11875), pH 5.6-5.8 adjusted by KOH] followed by stratification for
537 1-4 days in the dark at 4°C. Plates were placed vertically in a growth chamber [22°C, 16
538 h light/8 h dark (long-day) or 8 h light/16 h dark (short-day), illuminated with daylight
539 white fluorescent lamps (2 lamps/side)]. Seedlings were then transplanted into a soli
540 mixture [50% (v/v) Super Mix A (Sakata Seed), 50% (v/v) Vermiculite G20 (Nittai)] and
541 cultivated in either a growth chamber [22°C, 60% RH, 8 h light/16 h dark, illuminated

542 with daylight white fluorescent lamps (2 lamps/side)] or a growth room [22°C, 30-70%
543 RH, 16 h light/8 h dark, illuminated with daylight white fluorescent lamps (4
544 lamps/shelf)]. Plants were irrigated with either tap water or a modified Hoagland solution
545 [1.67 mM KNO_3, 0.67 mM $MgSO_4$, 5.21 μM KH_2PO_4, 28.3 μM KCl, 15.5 μM H_3BO_4,
546 3.07 μM $MnCl_2$, 0.28 μM $ZnSO_4$, 0.11 μM $CuSO_4$, 13.3 μg/L 80% molybdic acid
547 (FUJIFILM Wako Pure Chemical, Cat# 134-03332), 1.67 mM $Ca(NO_3)_2$, 46.3 μM
548 Fe(III)-EDTA (Dojindo, Cat# 345-01245)].
549
550 For general cultivation, 2-week-old seedings were transplanted and grown under long-
551 day conditions with irrigation using the modified Hoagland solution. For experiments
552 using 5-week-old plants, 2-week-old seedlings were transplanted and grown under short-
553 day conditions with irrigation using the modified Hoagland solution. For experiments
554 using 2-week-old plants, 4-day-old seedlings were transplanted and grown under long-
555 day conditions with irrigation using tap water.
556
557 **Plasmid construction**
558 For the generation of Arabidopsis transgenic plants, the promoter region (-2776 bp to -1
559 bp relative to the start codon) and the genomic complementation sequence (-2776 to
560 +1930 bp relative to the start codon) of *CYP707A3* were amplified from Arabidopsis WT
561 genomic DNA. The full-length coding sequences (excluding the stop codon) of AvrPtoB
562 and AvrPto were amplified from *Pst* DC3000 genomic DNA. A deletion of the CGCG
563 boxes in the *CYP707A3* promoter (-2220 bp to -2150 bp relative to the start codon) and
564 the AvrPtoB F479A substitution were introduced by overlap extension PCR. PCR
565 amplifications were performed using PrimeSTAR GXL DNA Polymerase (Takara Bio,
566 Cat# R050A). Amplified products were cloned into pENTR/D-TOPO using either the
567 pENTR/D-TOPO Cloning Kit (Thermo Scientific, Cat# K240020SP) or the In-Fusion
568 Snap Assembly Master Mix (Takara Bio, Cat# 638948). The resulting entry clones were
569 verified by Sanger sequencing with the BigDye Terminator v3.1 Cycle Sequencing Kit
570 (Applied Biosystems, Cat# 4337455) and recombined with destination vectors using
571 Gateway LR Clonase II Enzyme mix (Invitrogen, Cat# 11791020). The following
572 destination vectors were used: pGWB533[68] for GUS reporter constructs, pGWB501 (C-
573 3×FLAG) for *CYP707A3* complementation constructs, and pTA70001-DEST (Addgene,

574 Cat# 71745) for DEX-inducible constructs.
575
576 The pGWB501 (C-3×FLAG) vector was generated by cloning the 3×FLAG tag coding
577 sequence from pAMPAT-GW-3×FLAG[69] into the AfeI site of pGWB501[68] using In-
578 Fusion Snap Assembly Master Mix. For constructs encoding C-terminally 3×FLAG-
579 tagged AvrPtoB, AvrPto, and AvrPtoB-F479A, entry clones were recombined with
580 pAMPAT-GW-3×FLAG, and the resulting coding sequences were subsequently cloned
581 into pENTR/D-TOPO.
582
583 For the generation of Pst DC3000 mutant strains, the flanking 1 kb regions upstream and
584 downstream of either *avrPtoB* or *avrPto* were amplified from *Pst* DC3000 genomic DNA
585 by PCR using PrimeSTAR GXL DNA Polymerase. Amplified fragments were assembled
586 and cloned into EcoRI- and XbaI-digested pK18mobsacB using In-Fusion Snap
587 Assembly Master Mix. The resulting constructs were verified by Sanger sequencing with
588 the BigDye Terminator v3.1 Cycle Sequencing Kit.
589
590 All cloning procedures were performed according to the manufacturer's instructions.
591 Plasmids generated in this study and the primers for cloning are listed in Supplementary
592 Tables 5 and 6, respectively.
593
594 **Generation of Arabidopsis transgenic plants**
595 Expression vectors were introduced into *Agrobacterium tumefaciens* strain
596 GV3101::pMP90 by electroporation. Transgenic plants were generated by transforming
597 WT or *cyp707a3* mutant plants using the floral dip method[70]. For the *CYP707A3*
598 complementation experiments, T2 segregating lines were analyzed, whereas T3 or T4
599 homozygous lines were selected and used for all other experiments. The transgenic plants
600 used in this study are listed in Supplementary Table 4.
601
602 **Generation of *Pst* DC3000 mutant strains**
603 *Pst* DC3000 mutant strains lacking either *avrPtoB* or *avrPto* were generated by
604 introducing the pK18mobsacB-based constructs into *Pst* DC3000, as previously
605 described[71]. Deletions of *avrPtoB* and *avrPto* were verified by PCR using EmeraldAmp

606 MAX PCR Master Mix (Takara Bio, Cat# RR320A) and Sanger sequencing with the
607 BigDye Terminator v3.1 Cycle Sequencing Kit.. The primers used for PCR and Sanger
608 sequencing are listed in Supplementary Table 6.
609
610 **Chemicals**
611 The following stock solutions were prepared and stored at −30°C: $LaCl_3$ (FUJIFILM
612 Wako Pure Chemical, Cat# 123-04222), 1 M in water; $GdCl_3$ (FUJIFILM Wako Pure
613 Chemical, Cat# 078-02661), 1 M in water; Acetosyringone (FUJIFILM Wako Pure
614 Chemical, Cat# 320-29611), 100 mM in DMSO; Dexamethasone (DEX) (FUJIFILM
615 Wako Pure Chemical, Cat# 047-18863), 10 mM in ethanol.
616
617 **Humidity treatment**
618 High humidity treatment was performed by adding approximately 200 mL of modified
619 Hoagland solution or tap water (for 2-week-old plants grown under long-day conditions)
620 to a plastic container (Daiso, Cat# 4550480269726), spraying tap water onto the container
621 walls, placing the plants inside, sealing the container with plastic wrap, and immediately
622 returning it to the growth conditions. Moderate humidity treatment was performed by
623 adding approximately 500 mL of modified Hoagland solution or tap water (for 2-week-
624 old plants grown under long-day conditions) to a plastic tray (As One, Cat# 1-4618-01),
625 placing the plants inside, and immediately returning it to the growth conditions.
626
627 For inhibitor treatments and *Pst* DC3000 inoculation experiments, the indicated solutions
628 were infiltrated into three leaves per 5-week-old WT plant using a needleless syringe
629 (Terumo, Cat# SS-01T). Excess solution on the leaf surfaces was gently removed using
630 tissue paper (Elleair, Cat# DSI20703128). The infiltrated plants were maintained under
631 their growth conditions for 24 h (for inhibitor treatments) or 8 h (for *Pst* DC3000
632 inoculation), followed by humidity treatment. During *Pst* DC3000 inoculation
633 experiments, lights were kept on continuously from inoculation until sampling.
634
635 **Agrobacterium-mediated transient expression**
636 Agrobacterium-mediated transient expression was performed as previously described[72]
637 with minor modifications. *Agrobacterium tumefaciens* strain GV3101::pMP90 carrying

638 the relevant expression vectors was cultured overnight at 28°C with shaking (180 rpm) in
639 2×YT liquid medium [1% (w/v) yeast extract, 1.6% (w/v) tryptone, 0.5% (w/v) NaCl]
640 supplemented with 50 μg/mL gentamicin and 100 μg/mL spectinomycin. Bacterial cells
641 were collected by centrifugation at 2,000 *g* for 10 min at 25°C, washed once with sterile
642 water, and resuspended in sterile water to an OD_{600} of 0.05. Acetosyringone (100 mM
643 stock solution) was added to the suspension to a final concentration of 100 μM.
644
645 The bacterial suspensions were infiltrated into three leaves per 5-week-old *NahG* plant
646 using a needleless syringe. Excess solution on the leaf surfaces was gently removed using
647 tissue paper. The infiltrated plants were maintained under their growth conditions for
648 approximately 48 h before humidity treatment.
649
650 ***Pst* DC3000 inoculation assays**
651 The following *Pst* DC3000 strain were used in this study: WT, Δ*hrcC*[73], Δ28E[36],
652 Δ*avrPtoB* Δ*avrPto*[38], Δ*avrPtoB*, and Δ*avrPto*. Strains were cultured overnight at 28°C
653 with shaking (180 rpm) in King's B liquid medium [2% (w/v) Bacto Proteose Peptone
654 No. 3 (Gibco, Cat# 211693), 0.15% (w/v) K_2HPO4, 1% (v/v) glycerol, 5 mM $MgSO_4$]
655 supplemented with 50 μg/mL rifampicin and additional antibiotics as appropriate.
656 Bacterial cells were collected by centrifugation at 2,000 *g* for 10 min at 25°C, washed
657 once with sterile water, and resuspended in sterile water to the OD_{600} values indicated in
658 figure legends.
659
660 Bacterial suspensions were infiltrated into three leaves per plant using a needleless
661 syringe. Excess solution on the leaf surfaces was gently removed using tissue paper.
662 Infiltrated plants were maintained under their respective growth conditions for the
663 indicated time. To ensure high humidity (~95% RH), infiltrated plants were covered with
664 a plastic container as described in humidity treatment.
665
666 For water-soaking assays, the abaxial sides of infiltrated leaves were photographed at 1
667 day post-infiltration (dpi). The number of leaves exhibiting water-soaking was recorded,
668 or the water-soaked area relative to total leaf area was quantified using Image J software
669 (https://imagej.net/ij/). For growth assays, three inoculated leaves were collected from

670 three different plants at the indicated dpi. Leaves were homogenized in 1 mL sterile water,
671 and 10 uL aliquots of serial dilutions (10^{-1} to 10^{-8}) were spotted onto NYGA medium
672 [0.5% (w/v) Bacto Peptone (Gibco, Cat# 211677), 0.3% (w/v) yeast extract (Nacalai
673 Tesque, Cat# 15838-45), 2% (v/v) glycerol. 1.5% agar (Nacalai Tesque, Cat# 01162-15)]
674 supplemented with 50 μg/mL rifampicin. Colony-forming units (CFUs) were determined
675 after 2 days of incubation at 28°C.
676
677 **RT-qPCR**
678 Total RNA was extracted from three leaves or a single shoot segment using Sepasol-RNA
679 I Super G (Nacalai Tesque, Cat# 09379-55), followed by DNase treatment and reverse
680 transcription (RT) with the PrimeScript RT reagent Kit with the gDNA Eraser (Takara,
681 Cat# RR047B), according to the manufacturer's instructions. Quantitative PCR (qPCR)
682 was performed using Power SYBR Green PCR Master Mix (Applied Biosystems, Cat#
683 4368702) on a Thermal Cycler Dice Real Time System III (Takara, Cat# TP950). Gene
684 expression levels were calculated using the ΔΔCt method, with normalization to *ACTIN2*
685 as an internal reference. Primers used for qPCR are listed in Supplementary Table 6.
686
687 **Immunoblotting**
688 Frozen plant tissue (three leaves per sample) was ground into a fine powder and
689 resuspended in protein extraction buffer [62.5 mM Tris-HCl (pH 6.8), 10% glycerol, 2%
690 SDS, 5% (v/v) 2-mercaptoethanol, 0.02% bromophenol blue] supplemented with 1 mM
691 EDTA (pH 8.0) and protease inhibitor cocktail (Roche, Cat# 11873580001). The buffer
692 was added at a ratio of 3 μL per mg of tissue weight. Extracts were incubated at 95°C for
693 5 min and subsequently centrifuged at 20,000 *g* for 10 min at 25°C, and the supernatants
694 were collected.
695
696 Proteins were separated on a 10% polyacrylamide gel and transferred to a PVDF
697 membrane (Millipore, Cat# IPVH00010). The membrane was blocked 2% (w/v) skim
698 milk (Nacalai Tesque, Cat# 31149-75) in TBS-T [25 mM Tris, 192 mM glycine, 0.1%
699 (v/v) Tween-20] for 1 h at 25°C with agitation, rinsed once with deionized water, and
700 once with TBS-T. The blocked membrane was incubated overnight at 4°C with the
701 primary antibody solution under agitation, rinsed five times with deionized water, and

702 washed once in TBS-T for 5 min at 25°C. Subsequently, the membrane was incubated
703 with the secondary antibody solution for 1 h at 25°C with agitation, rinsed five times with
704 deionized water, and washed once with TBS-T for 5 min at 25°C.
705
706 Chemiluminescent detection was performed using Chemi-Lumi One L (Nacalai Tesque,
707 Cat# 07880) and a FUSION FX imaging system (Vilber). The following antibodies were
708 used for immunoblotting: anti-FLAG (Sigma-Aldrich, Cat# F1804; 1:5000 dilution), anti-
709 GFP (MBL, Cat# 598; 1:5000 dilution), anti-mouse IgG HRP-linked (Cell Signaling
710 Technology, Cat# 7076; 1:5000 dilution), and anti-rabbit IgG HRP-linked (Cell Signaling
711 Technology, Cat# 7074; 1:5000 dilution). All antibodies were diluted in TBS-T.
712
713 **Phytohormone quantification**
714 SA, ABA, and JA-Ile were extracted and purified from freeze-dried samples as previously
715 described[74]. For hormone measurement, isotope-labeled internal standards were added at
716 the initial extraction procedure. Plant hormones were analyzed by a LC-MS/MS system
717 (ACQUITY UPLC I-Class PLUS FTN/Xevo TQ-S micro; Waters) equipped with a short
718 ODS column (TSKgel ODS-120H 2.0 mm I.D. x 5 cm, 1.9 µm; TOSHO) or a long ODS
719 column (TSKgel ODS-120H 2.0 mm I.D. x 15 cm, 1.9 µm; TOSHO). A binary solvent
720 system composed of 0.1% acetic acid (v/v) ACN (A) and 0.1% acetic acid (v/v) H_2O (B)
721 was used. SA, ABA, and JA-Ile were measured using the short ODS column, and
722 separation was performed at a flow rate of 0.2 mL/min with the following linear gradient
723 of solvent B: 0–2 min (1%–5%), 2–5 min (5%–15%), 5–25 min (15%–40%), 25.1–27
724 min (100%), and 27.1–30 min (1%). The retention times for each compound were as
725 follows: d_6-SA (7.39), SA (7.46), d_6-ABA (12.59), ABA (12.67), $^{13}C_6$-JA-Ile (21.64), and
726 JA-Ile (21.94). The MS/MS analysis was performed under the following conditions:
727 capillary (kV) = 1.00, source temperature (°C) = 150, desolvation temperature (°C) = 500,
728 cone gas flow (L/h) = 50, desolvation gas flow (L/h) = 1000. Ion mode was negative. The
729 MS/MS transitions (*m*/*z*) and collision energies (V) for each compound were as follows:
730 d_6-SA (142.1/98.0, 18V), SA (137.0/93.4, 18V), d_6-ABA (269.1/159.1, 8V), ABA
731 (263.1/153.1, 8V), $^{13}C_6$-JA-Ile (328.2/136.1, 20V), and JA-Ile (322.2/130.1, 20V).
732
733 **Stomatal aperture measurement**

734 Following humidity treatment, detached leaves were immediately immersed in 4% (v/v)
735 formaldehyde and incubated overnight at 25°C. Images of stomata on the abaxial leaf
736 surface were captured using a Leica DMI6000 B microscope equipped with 10× objective
737 lens. Stomatal aperture was quantified using Image J software.
738
739 **Real-time cytosolic Ca^{2+} imaging**
740 Real-time cytosolic Ca^{2+} imaging of whole plants expressing GCaMP3 was performed as
741 described previously[75,76].
742
743 **RNA-sequencing and data analysis**
744 Total RNA was extracted from three leaves and treated with DNase using the NucleoSpin
745 RNA Plant kit (Macherey-Nagel, Cat# 740949.50) according to the manufacturer's
746 instruction. RNA quality was assessed using a bioanalyzer (Agilent Technologies).
747
748 Each raw read data stored in DDBJ with accession numbers DRR545835 to DRR545846
749 was generated and analyzed as follows. Each RNA library was prepared from 1000 ng of
750 total RNA using the NEBNext Ultra II RNA Library Prep Kit for Illumina (New England
751 Biolabs, Cat# E7770) according to the manufacturer's instruction. PCR for library
752 amplification was performed for 7 cycles. The average length of the library was 350 bp,
753 as measured by a bioanalyzer. Concentrations were measured by Kapa Library
754 Quantification Kit (Kapa Biosystems, Cat# KK4824), each sample was diluted to 10 nM,
755 and equal volumes were mixed. Single reads of 75 bp were obtained using a NextSeq 500
756 system (Illumina). CLC genomics workbench version 21 (Qiagen) was used to trim raw
757 reads and map to the TAIR10 Arabidopsis genome (https://www.arabidopsis.org/). In
758 trimming, the following parameters were changed (quality limit = 0.001, number of 5′
759 terminal nucleotides =15, number of 3′ terminal nucleotides = 5, and minimum number
760 of nucleotides in reads =25) and other options were default values. In mapping, all options
761 were default values.
762
763 The generation and analysis of each raw read data stored in DDBJ with accession numbers
764 DRR545847 to DRR545870 differs from the above analysis in three points. 1) Each
765 library was prepared from 500 ng total RNA using the NEBNext Ultra II Directional RNA

Library Prep Kit for Illumina (New England Biolabs, Cat# 7760). PCR for library amplification was performed for 8 cycles. Each sample was diluted to 4 nM, and equal volumes were mixed. 2) Single reads of 100 bp were obtained using a NextSeq 1000 system (Illumina). 3) CLC genomics workbench version 24 (Qiagen) was used for reads trimming and mapping. In trimming and mapping, the following parameters were changed (minimum number of nucleotides in reads = 40, and strand setting = Revers). All other methods, numbers, options are the same as above analysis.

The obtained read counts were processed and analyzed using iDEP 2.01 (https://bioinformatics.sdstate.edu/idep/) with default settings. Gene Ontology and *cis*-regulatory enrichment analyses were performed using ShinyGO 0.81 (https://bioinformatics.sdstate.edu/go/) with default settings. For *cis*-regulatory enrichment analysis, the AGRIS database was used as the pathway reference.

Accession numbers

The gene sequences analyzed in this study were obtained from The Arabidopsis Information Resource (https://www.arabidopsis.org/) and The Pseudomonas Genome Database (https://www.pseudomonas.com/), under the accession numbers listed in Supplementary Table 7.

Statistical analysis

All data, except RNA-seq, were analyzed using GraphPad Prism 10 software (https://www.graphpad.com/features). No statistical methods were used to predetermine sample size, and no data were excluded from analyses. Experiments were not randomized, and investigators were not blinded to group allocation or outcome assessment. Statistical comparisons were performed using two-tailed Welch's t test, or one-way or two-way ANOVA followed by Tukey's multiple comparison test, as specified in the figure legends.

Data availability

The raw RNA sequencing data have been submitted in the DDJB database under accession numbers DRR545835 to DRR545870.

Acknowledgements

We thank Chika Tateda, Mie Matsubara, Taiga Ishihara, Natsuki Tsuchida, and Temma Takazawa (Nara Institute of Science and Technology) for technical assistance; Yuri Kanno (RIKEN CSRS) for supporting plant hormone analysis; Akira Mine (Kyoto University) for *cyp707a* seeds; Atsushi Takemiya (Yamaguchi University) for *ost2-3D* seeds; Michael F. Thomashow (Michigan State University) for *camta* seeds; Alan Collmer (Cornell University) for *Pst* DC3000 strains. We also thank the NAIST Life Science Collaboration Center (LiSCo) for supporting this study. This work was supported in part by JSPS KAKENHI Grant Numbers 21K14829 (S.Y.), 24H00565 (M.T.) and 21H02507 (Y.S.), JST ACT-X Grant Number JPMJAX22BN (S.Y.), ERATO Grant Number JPMJER2403 (M.T.), Cooperative Research Grant of the Genome Research for BioResource, NODAI Genome Research Center, Tokyo University of Agriculture (S.Y.), and Institute for Fermentation, Osaka Grant Number G-2025-2-089 (S.Y.).

Author contributions

S.Y. and Y.S. conceived the study. S.Y. designed the research, conducted most of the experiments, and analyzed the data. A.R, T.H., and S.U. performed part of the RT-qPCR and *Pst* DC3000 inoculation assay. Y.W., Y.T., and M.O. performed phytohormone quantification. H.I., R.Suzuki, and M.T performed GCaMP3 imaging. A.S., R.Sk, and I.Y. performed RNA-sequencing. S.Y. and Y.S. wrote the manuscript with input from the other authors.

Competing interests

The authors declare no competing interests.

References

1 Xin, X. F., Kvitko, B. & He, S. Y. Pseudomonas syringae: what it takes to be a pathogen. *Nat. Rev. Microbiol.* **16**, 316-328 (2018).

2 Boutrot, F. & Zipfel, C. Function, Discovery, and Exploitation of Plant Pattern Recognition Receptors for Broad-Spectrum Disease Resistance. *Annu. Rev. Phytopathol.* **55**, 257-286 (2017).

3 DeFalco, T. A. & Zipfel, C. Molecular mechanisms of early plant pattern-

830 triggered immune signaling. *Mol. Cell* **81**, 3449-3467 (2021).
831 4 Saijo, Y., Loo, E. P. & Yasuda, S. Pattern recognition receptors and signaling in
832 plant-microbe interactions. *Plant J.* **93**, 592-613 (2018).
833 5 Wei, H. L. *et al.* Pseudomonas syringae pv. tomato DC3000 Type III Secretion
834 Effector Polymutants Reveal an Interplay between HopAD1 and AvrPtoB. *Cell*
835 *Host Microbe* **17** (2015).
836 6 Roussin-Léveillée, C., Mackey, D., Ekanayake, G., Gohmann, R. & Moffett, P.
837 Extracellular niche establishment by plant pathogens. *Nat. Rev. Microbiol.* **22**,
838 360-372 (2024).
839 7 Panchal, S. *et al.* Regulation of Stomatal Defense by Air Relative Humidity.
840 *Plant Physiol.* **172**, 2021-2032 (2016).
841 8 Xin, X. F. *et al.* Bacteria establish an aqueous living space in plants crucial for
842 virulence. *Nature* **539**, 524-529 (2016).
843 9 Hu, Y. *et al.* Bacterial effectors manipulate plant abscisic acid signaling for
844 creation of an aqueous apoplast. *Cell Host Microbe* **30**, 518-529 (2022).
845 10 Roussin-Léveillée, C. *et al.* Evolutionarily conserved bacterial effectors hijack
846 abscisic acid signaling to induce an aqueous environment in the apoplast. *Cell*
847 *Host Microbe* **30**, 489-501 (2022).
848 11 Waadt, R. *et al.* Plant hormone regulation of abiotic stress responses. *Nat. Rev.*
849 *Mol. Cell Biol.* **23**, 680-694 (2022).
850 12 Zhang, D., Tian, C., Yin, K., Wang, W. & Qiu, J. L. Postinvasive Bacterial
851 Resistance Conferred by Open Stomata in Rice. *Mol. Plant Microbe Interact.* **32**,
852 255-266 (2019).
853 13 Peng, Z. *et al.* Xanthomonas translucens commandeers the host rate-limiting
854 step in ABA biosynthesis for disease susceptibility. *Proc. Natl Acad. Sci. USA*
855 **116**, 20938-20946 (2019).
856 14 You, Y. *et al.* The eINTACT system dissects bacterial exploitation of plant
857 osmosignalling to enhance virulence. *Nat. Plants* **9**, 128-141 (2023).
858 15 Wu, J. *et al.* CURLY LEAF modulates apoplast liquid water status in
859 Arabidopsis leaves. *Plant Physiol.* **193**, 792-808 (2023).
860 16 Lajeunesse, G. *et al.* Light prevents pathogen-induced aqueous
861 microenvironments via potentiation of salicylic acid signaling. *Nat. Commun.*
862 **14**, 713 (2023).
863 17 Okamoto, M. *et al.* High humidity induces abscisic acid 8'-hydroxylase in
864 stomata and vasculature to regulate local and systemic abscisic acid responses in
865 Arabidopsis. *Plant Physiol.* **149**, 825-834 (2009).

18 Kim, H., Yu, S. I., Jung, S. H., Lee, B. H. & Suh, M. C. The F-Box Protein SAGL1 and ECERIFERUM3 Regulate Cuticular Wax Biosynthesis in Response to Changes in Humidity in Arabidopsis. *Plant Cell* **31**, 2223-2240 (2019).

19 Jiang, Z. *et al.* Ethylene signaling modulates air humidity responses in plants. *Plant J.* **117**, 653-668 (2024).

20 Nambara, E. & Marion-Poll, A. Abscisic acid biosynthesis and catabolism. *Annu. Rev. Plant Biol.* **56**, 165-185 (2005).

21 Yao, L. *et al.* High air humidity dampens salicylic acid pathway and NPR1 function to promote plant disease. *EMBO J.* **42**, e113499 (2023).

22 Yamauchi, S. *et al.* The Plasma Membrane H^+-ATPase AHA1 Plays a Major Role in Stomatal Opening in Response to Blue Light. *Plant Physiol.* **171**, 2731-2743 (2016).

23 Yasuda, M. *et al.* Antagonistic interaction between systemic acquired resistance and the abscisic acid-mediated abiotic stress response in Arabidopsis. *Plant Cell* **20**, 1678-1692 (2008).

24 de Torres Zabala, M., Bennett, M. H., Truman, W. H. & Grant, M. R. Antagonism between salicylic and abscisic acid reflects early host-pathogen conflict and moulds plant defence responses. *Plant J.* **59**, 375-386 (2009).

25 Melotto, M., Zhang, L., Oblessuc, P. R. & He, S. Y. Stomatal Defense a Decade Later. *Plant Physiol.* **174**, 561-571 (2017).

26 Rekhter, D. *et al.* Isochorismate-derived biosynthesis of the plant stress hormone salicylic acid. *Science* **365**, 498-502 (2019).

27 Seo, M. *et al.* The Arabidopsis aldehyde oxidase 3 (AAO3) gene product catalyzes the final step in abscisic acid biosynthesis in leaves. *Proc. Natl Acad. Sci. USA* **97**, 12908-12913 (2000).

28 Yuan, M. *et al.* Pattern-recognition receptors are required for NLR-mediated plant immunity. *Nature* **592**, 105-109 (2021).

29 Wang, Y. *et al*. A calmodulin-binding transcription factor links calcium signaling to antiviral RNAi defense in plants. *Cell Host Microbe*. **29**, 1393-1406 (2021).

30 DeFalco, T. A., Moeder, W. & Yoshioka, K. Opening the Gates: Insights into Cyclic Nucleotide-Gated Channel-Mediated Signaling. *Trends Plant Sci.* **21**, 903-906 (2016).

31 Kim, Y., Park, S., Gilmour, S. J. & Thomashow, M. F. Roles of CAMTA transcription factors and salicylic acid in configuring the low-temperature transcriptome and freezing tolerance of Arabidopsis. *Plant J.* **75**, 364-376 (2013).

902 32 Kidokoro, S. *et al.* Different Cold-Signaling Pathways Function in the
903 Responses to Rapid and Gradual Decreases in Temperature. *Plant Cell* **29**, 760-
904 774 (2017).
905 33 Darwish, E. *et al.* Touch signaling and thigmomorphogenesis are regulated by
906 complementary CAMTA3- and JA-dependent pathways. *Sci. Adv.* **8**, eabm2091
907 (2022).
908 34 Matsumura, M. *et al.* Mechanosensory trichome cells evoke a mechanical
909 stimuli-induced immune response in Arabidopsis thaliana. *Nat. Commun.* **13**,
910 1216 (2022).
911 35 Kim, Y. S. *et al.* CAMTA-Mediated Regulation of Salicylic Acid Immunity
912 Pathway Genes in Arabidopsis Exposed to Low Temperature and Pathogen
913 Infection. *Plant Cell* **29**, 2465-2477 (2017).
914 36 Cunnac, S. *et al.* Genetic disassembly and combinatorial reassembly identify a
915 minimal functional repertoire of type III effectors in Pseudomonas syringae.
916 *Proc. Natl Acad. Sci. USA* **108**, 2975-2980 (2011).
917 37 de Torres-Zabala, M. *et al.* Pseudomonas syringae pv. tomato hijacks the
918 Arabidopsis abscisic acid signalling pathway to cause disease. *EMBO J.* **26**,
919 1434-1443 (2007).
920 38 Lin, N. C. & Martin, G. B. An avrPto/avrPtoB mutant of Pseudomonas syringae
921 pv. tomato DC3000 does not elicit Pto-mediated resistance and is less virulent
922 on tomato. *Mol. Plant Microbe Interact.* **18**, 43-51 (2005).
923 39 Janjusevic, R., Abramovitch, R. B., Martin, G. B. & Stebbins, C. E. A bacterial
924 inhibitor of host programmed cell death defenses is an E3 ubiquitin ligase.
925 *Science* **311**, 222-226 (2006).
926 40 Mwimba, M. *et al.* Daily humidity oscillation regulates the circadian clock to
927 influence Plant Physiol.. *Nat. Commun.* **9**, 4290 (2018).
928 41 Rowe, J. *et al.* Next-generation ABACUS biosensors reveal cellular ABA
929 dynamics driving root growth at low aerial humidity. *Nat. Plants* **9**, 1103-1115
930 (2023).
931 42 Tulva, I., Koolmeister, K. & Hõrak, H. Low relative air humidity and increased
932 stomatal density independently hamper growth in young Arabidopsis. *Plant J.*
933 **119**, 2718-2736 (2024).
934 43 Romero, F. *et al.* Humidity and high temperature are important for predicting
935 fungal disease outbreaks worldwide. *New Phytol.* **234**, 1553-1556 (2022).
936 44 L'Haridon, F. *et al.* A permeable cuticle is associated with the release of reactive
937 oxygen species and induction of innate immunity. *PLoS Pathog.* **7**, e1002148

(2011).
45 Cui, F. *et al.* Dissecting Abscisic Acid Signaling Pathways Involved in Cuticle Formation. *Mol. Plant* **9**, 926-938 (2016).
46 Hsu, F. C. *et al.* Submergence confers immunity mediated by the WRKY22 transcription factor in Arabidopsis. *Plant Cell* **25**, 2699-2713 (2013).
47 Ding, Y., Dommel, M. & Mou, Z. Abscisic acid promotes proteasome-mediated degradation of the transcription coactivator NPR1 in Arabidopsis thaliana. *Plant J.* **86**, 20-34 (2016).
48 Berens, M. L. *et al.* Balancing trade-offs between biotic and abiotic stress responses through leaf age-dependent variation in stress hormone cross-talk. *Proc. Natl Acad. Sci. USA* **116**, 2364-2373 (2019).
49 Umezawa, T. *et al.* CYP707A3, a major ABA 8'-hydroxylase involved in dehydration and rehydration response in Arabidopsis thaliana. *Plant J.* **46**, 171-182 (2006).
50 Zhang, Y. *et al.* Control of salicylic acid synthesis and systemic acquired resistance by two members of a plant-specific family of transcription factors. *Proc. Natl Acad. Sci. USA* **107**, 18220-18225 (2010).
51 Wang, L. *et al.* CBP60g and SARD1 play partially redundant critical roles in salicylic acid signaling. *Plant J.* **67**, 1029-1041 (2011).
52 Zhang, B. *et al.* The mitochondrial outer membrane AAA ATPase AtOM66 affects cell death and pathogen resistance in Arabidopsis thaliana. *Plant J.* **80**, 709-727 (2014).
53 Kemppinen, J., Pollmeier, M., Ehonen, S., Brosché, M. & Sierla, M. Water immunity overrides stomatal immunity in plant resistance to *Pseudomonas syringae*. *Plant Physiol*. **198**, kiaf127 (2025).
54 Liu, Y., Mahmud, M. R., Xu, N. & Liu, J. The Pseudomonas syringae effector AvrPtoB targets abscisic acid signaling pathway to promote its virulence in Arabidopsis. *Phytopathol. Res.* **4**, 5 (2022).
55 Shan, L. *et al.* Bacterial effectors target the common signaling partner BAK1 to disrupt multiple MAMP receptor-signaling complexes and impede plant immunity. *Cell Host Microbe* **4**, 17-27 (2008).
56 Göhre, V. *et al.* Plant pattern-recognition receptor FLS2 is directed for degradation by the bacterial ubiquitin ligase AvrPtoB. *Curr. Biol.* **18**, 1824-1832 (2008).
57 Gimenez-Ibanez, S. *et al.* AvrPtoB targets the LysM receptor kinase CERK1 to promote bacterial virulence on plants. *Curr. Biol.* **19**, 423-429 (2009).

58 Chen, H. *et al.* A Bacterial Type III Effector Targets the Master Regulator of Salicylic Acid Signaling, NPR1, to Subvert Plant Immunity. *Cell Host Microbe* **22**, 777-788 (2017).

59 Wang, W., Liu, N., Gao, C., Rui, L. & Tang, D. The Pseudomonas Syringae Effector AvrPtoB Associates With and Ubiquitinates Arabidopsis Exocyst Subunit EXO70B1. *Front. Plant Sci.* **10**, 1027 (2019).

60 Wang, M. Y. *et al.* The plant immune receptor SNC1 monitors helper NLRs targeted by a bacterial effector. *Cell Host Microbe* **31**, 1792-1803 (2023).

61 Hussain, S. *et al.* Calcium signaling triggers early high humidity responses in Arabidopsis thaliana. *Proc. Natl Acad. Sci. USA* **121**, e2416270121 (2024).

62 Lee, S. *et al.* Oomycete effector AVRblb2 targets cyclic nucleotide-gated channels through calcium sensors to suppress pattern-triggered immunity. *New Phytol.* **241**, 1277-1291 (2024).

63 Jing, B. *et al.* Brush and spray: a high-throughput systemic acquired resistance assay suitable for large-scale genetic screening. *Plant Physiol.* **157**, 973-980 (2011).

64 Nie, H. *et al.* SR1, a calmodulin-binding transcription factor, modulates plant defense and ethylene-induced senescence by directly regulating NDR1 and EIN3. *Plant Physiol.* **158**, 1847-1859 (2012).

65 Jacob, F. *et al.* A dominant-interfering camta3 mutation compromises primary transcriptional outputs mediated by both cell surface and intracellular immune receptors in Arabidopsis thaliana. *New Phytol.* **217**, 1667-1680 (2018).

66 Lolle, S. *et al.* Matching NLR Immune Receptors to Autoimmunity in camta3 Mutants Using Antimorphic NLR Alleles. *Cell Host Microbe* **21**, 518-529 (2017).

67 Goel, A. K. *et al.* The Pseudomonas syringae type III effector HopAM1 enhances virulence on water-stressed plants. *Mol. Plant Microbe Interact.* **21**, 361-370 (2008).

68 Nakagawa, T. *et al.* Improved Gateway binary vectors: high-performance vectors for creation of fusion constructs in transgenic analysis of plants. *Biosci. Biotechnol. Biochem.* **71**, 2095-2100 (2007).

69 Yamada, K. *et al.* Danger peptide receptor signaling in plants ensures basal immunity upon pathogen-induced depletion of BAK1. *EMBO J.* **35**, 46-61 (2016).

70 Zhang, X., Henriques, R., Lin, S. S., Niu, Q. W. & Chua, N. H. Agrobacterium-mediated transformation of Arabidopsis thaliana using the floral dip method.

1010 *Nat. Protoc.* **1**, 641-646 (2006).
1011 71 Matsumoto, A., Schlüter, T., Melkonian, K., Takeda, A., Nakagami, H., Mine, A.
1012 A versatile Tn7 transposon-based bioluminescence tagging tool for quantitative
1013 and spatial detection of bacteria in plants. *Plant Commun*. **3**, 100227 (2021).
1014 72 Rosas-Díaz, T. *et al.* Arabidopsis NahG Plants as a Suitable and Efficient System
1015 for Transient Expression using Agrobacterium tumefaciens. *Mol. Plant* **10**, 353-
1016 356 (2017).
1017 73 Wei, W. *et al.* The gene coding for the Hrp pilus structural protein is required for
1018 type III secretion of Hrp and Avr proteins in Pseudomonas syringae pv. tomato.
1019 *Proc. Natl Acad. Sci. USA* **97**, 2247-2252 (2000).
1020 74 Sato, Y. *et al.* Temporal dynamics of N-hydroxypipecolic acid and salicylic acid
1021 pathways in the disease response to powdery mildew in wheat. *Biochem.*
1022 *Biophys. Res. Commun.* **734**, 150624 (2024).
1023 75 Toyota, M. *et al.* Glutamate triggers long-distance, calcium-based plant defense
1024 signaling. *Science* **361**, 1112-1115 (2018).
1025 76 Aratani, Y., Uemura, T., Hagihara, T., Matsui, K. & Toyota, M. Green leaf
1026 volatile sensory calcium transduction in Arabidopsis. *Nat. Commun.* **14**, 6236
1027 (2023).
1028 77 Okamoto, M. *et al.* CYP707A1 and CYP707A2, which encode abscisic acid 8'-
1029 hydroxylases, are indispensable for proper control of seed dormancy and
1030 germination in Arabidopsis. *Plant Physiol.* **141**, 97-107 (2006).
1031 78 Kushiro, T. *et al.* The Arabidopsis cytochrome P450 CYP707A encodes ABA 8'-
1032 hydroxylases: key enzymes in ABA catabolism. *EMBO J.* **23**, 1647-1656 (2004).
1033 79 Wildermuth, M. C., Dewdney, J., Wu, G. & Ausubel, F. M. Isochorismate
1034 synthase is required to synthesize salicylic acid for plant defence. *Nature* **414**,
1035 562-565 (2001).
1036 80 Seo, M. *et al.* Comparative studies on the Arabidopsis aldehyde oxidase (AAO)
1037 gene family revealed a major role of AAO3 in ABA biosynthesis in seeds. *Plant*
1038 *Cell Physiol.* **45**, 1694-1703 (2004).
1039 81 Schwessinger, B. *et al.* Phosphorylation-dependent differential regulation of
1040 plant growth, cell death, and innate immunity by the regulatory receptor-like
1041 kinase BAK1. *PLoS Genet.* **7**, e1002046 (2011).
1042 82 He, K. *et al.* BAK1 and BKK1 regulate brassinosteroid-dependent growth and
1043 brassinosteroid-independent cell-death pathways. *Curr. Biol.* **17**, 1109-1115
1044 (2007).
1045 83 Miya, A. *et al.* CERK1, a LysM receptor kinase, is essential for chitin elicitor

signaling in Arabidopsis. *Proc. Natl Acad. Sci. USA* **104**, 19613-19618 (2007).

84 Yu, X. *et al.* The Receptor Kinases BAK1/SERK4 Regulate Ca^{2+} Channel-Mediated Cellular Homeostasis for Cell Death Containment. *Curr. Biol.* **29**, 3778-3790 (2019).

85 Clough, S. J. *et al.* The Arabidopsis dnd1 "defense, no death" gene encodes a mutated cyclic nucleotide-gated ion channel. *Proc. Natl Acad. Sci. USA* **97**, 9323-9328 (2000).

86 Gobert, A., Park, G., Amtmann, A., Sanders, D. & Maathuis, F. J. Arabidopsis thaliana cyclic nucleotide gated channel 3 forms a non-selective ion transporter involved in germination and cation transport. *J. Exp. Bot.* **57**, 791-800 (2006).

87 Jurkowski, G. I. *et al.* Arabidopsis DND2, a second cyclic nucleotide-gated ion channel gene for which mutation causes the "defense, no death" phenotype. *Mol. Plant Microbe Interact.* **17**, 511-520 (2004).

88 Tan, Y. Q. *et al.* Three CNGC Family Members, CNGC5, CNGC6, and CNGC9, Are Required for Constitutive Growth of Arabidopsis Root Hairs as Ca(2+)-Permeable Channels. *Plant Commun.* **1**, 100001 (2020).

89 Tunc-Ozdemir, M. *et al.* Cyclic nucleotide gated channels 7 and 8 are essential for male reproductive fertility. *PLoS One* **8**, e55277 (2013).

90 Yoshioka, K. *et al.* The chimeric Arabidopsis CYCLIC NUCLEOTIDE-GATED ION CHANNEL11/12 activates multiple pathogen resistance responses. *Plant Cell* **18**, 747-763 (2006).

91 Shih, H. W., DePew, C. L., Miller, N. D. & Monshausen, G. B. The Cyclic Nucleotide-Gated Channel CNGC14 Regulates Root Gravitropism in Arabidopsis thaliana. *Curr. Biol.* **25**, 3119-3125 (2015).

92 Moon, J. Y., Belloeil, C., Ianna, M. L. & Shin, R. Arabidopsis CNGC Family Members Contribute to Heavy Metal Ion Uptake in Plants. *Int. J. Mol. Sci.* **20**, 413 (2019).

93 Tunc-Ozdemir, M. *et al.* A cyclic nucleotide-gated channel (CNGC16) in pollen is critical for stress tolerance in pollen reproductive development. *Plant Physiol.* **161**, 1010-1020 (2013).

94 Ladwig, F. *et al.* Phytosulfokine Regulates Growth in Arabidopsis through a Response Module at the Plasma Membrane That Includes CYCLIC NUCLEOTIDE-GATED CHANNEL17, H^{+}-ATPase, and BAK1. *Plant Cell* **27**, 1718-1729 (2015).

95 Gao, Q. F. *et al.* Cyclic nucleotide-gated channel 18 is an essential Ca^{2+} channel in pollen tube tips for pollen tube guidance to ovules in Arabidopsis. *Proc. Natl*

1082 *Acad. Sci. USA* **113**, 3096-3101 (2016).
1083 96 Kugler, A., Köhler, B., Palme, K., Wolff, P. & Dietrich, P. Salt-dependent
1084 regulation of a CNG channel subfamily in Arabidopsis. *BMC Plant Biol.* **9**, 140
1085 (2009).
1086 97 Lawton, K. *et al.* Systemic acquired resistance in Arabidopsis requires salicylic
1087 acid but not ethylene. *Mol. Plant Microbe Interact.* **8**, 863-870 (1995).
1088 98 Doherty, C. J., Van Buskirk, H. A., Myers, S. J. & Thomashow, M. F. Roles for
1089 Arabidopsis CAMTA transcription factors in cold-regulated gene expression and
1090 freezing tolerance. *Plant Cell* **21**, 972-984 (2009).
1091 99 Gu, Y. & Innes, R. W. The KEEP ON GOING protein of Arabidopsis recruits the
1092 ENHANCED DISEASE RESISTANCE1 protein to trans-Golgi network/early
1093 endosome vesicles. *Plant Physiol.* **155**, 1827-1838 (2011).
1094

1095 **Fig. 1: *CYP707A3* is required for resistance to bacterial water-soaking under high**
1096 **humidity.**
1097 **a,** Expression levels of *CYP707A* genes in humidity-treated leaves. Wild-type (WT) plants
1098 were exposed to moderate humidity (MH) or high humidity (HH) for the indicated time.
1099 Bars represent means (n = 3). **b**, ABA levels in humidity-treated leaves. The indicated
1100 plants were exposed to MH or HH for 2 h. Bars represent means (n = 3). **c**, **d**, Water-
1101 soaking in *Pst* Δ*hrcC*-inoculated leaves. The indicated plants were infiltrated with *Pst*
1102 Δ*hrcC* (OD_{600} = 0.02) and maintained under MH or HH for 1 day. The number of water-
1103 soaked leaves was pooled from two independent experiments. **e**, Bacterial growth in *Pst*
1104 Δ*hrcC*-inoculated leaves. The indicated plants were infiltrated with *Pst* Δ*hrcC* (OD_{600} =
1105 0.02) and maintained under MH or HH for 3 days. Bars represent means (n = 6). Different
1106 letters indicate statistically significant differences ($P < 0.05$; two-way ANOVA followed
1107 by Tukey's test). dpi, days post-infiltration. Experiments in (**a**) and (**e**) were repeated twice
1108 with similar results.
1109

1110 **Fig. 2: *CYP707A3*-mediated water-soaking resistance depends on stomatal opening.**
1111 **a**, **b**, Representative images of stomata (**a**) and stomatal aperture (**b**) in humidity-treated
1112 leaves. The indicated plants were exposed to moderate humidity (MH) or high humidity
1113 (HH) for 1 h. Bars represent the median (n = 149-264). **c**, Water-soaking in *Pst* Δ*hrcC*-
1114 inoculated leaves. The indicated plants were infiltrated with *Pst* Δ*hrcC* (OD_{600} = 0.02)

1115 and maintained under HH for 1 day. The number of water-soaked leaves was pooled from
1116 two independent experiments. **d**, Bacterial growth in *Pst* Δ*hrcC*-inoculated leaves. The
1117 indicated plants were infiltrated with *Pst* Δ*hrcC* (OD_{600} = 0.02) and maintained under HH
1118 for 3 days. Bars represent means (n = 6). Different letters indicate statistically significant
1119 differences (P < 0.05; two-way ANOVA followed by Tukey's test in **b**; one-way ANOVA
1120 followed by Tukey's test in **d**). WT, wild-type; dpi, days post-infiltration. Experiments in
1121 (**b**) and (**d**) were repeated twice with similar results.
1122
1123 **Fig. 3: CAMTA binding motifs are overrepresented in early-phase high humidity-**
1124 **induced genes.**
1125 **a-c**, Transcriptome profiling of humidity-treated leaves by RNA-seq. Wild-type plants
1126 were exposed to moderate humidity (MH) or high humidity (HH) for the indicated time.
1127 **a**, Venn diagrams showing differentially expressed genes (DEGs) (fold change > 2; FDR
1128 < 0.05) at 0.5 h and 5 h after treatment. **b**, Principal component analysis (PCA) of
1129 transcriptomic data. **c**, K-means clustering of the 1000 most variable genes. **d**, Top 10
1130 enriched *cis*-regulatory elements among high humidity-induced genes identified in the
1131 clusters shown in (**c**).
1132
1133 **Fig. 4: CAMTA3 drives *CYP707A3* expression to promote resistance to bacterial**
1134 **water-soaking under high humidity.**
1135 **a**, Schematic diagram of the promoter regions of *CYP707A3* and *CYP707A1*, highlighting
1136 the CGCG box. **b**, *GUS* expression driven by the *CYP707A3* promoter, with or without
1137 CGCG boxes, in humidity-treated leaves. The indicated constructs were transiently
1138 expressed in *NahG* leaves via *Agrobacterium* infiltration. Infiltrated plants were
1139 maintained under moderate humidity (MH) for 24 h, then exposed to MH or high
1140 humidity (HH) for 0.5 h. Bars represent means (n = 3). **c**, **d**, Expression levels of
1141 *CYP707A3* and *CYP707A1* in humidity-treated leaves of *cngc* (**c**) and *camta3* (**d**) mutants.
1142 The indicated plants were exposed to MH or HH for 0.5 h. Bars represent means (n = 3).
1143 **e**, ABA levels in humidity-treated leaves. The indicated plants were exposed to MH or
1144 HH for 2 h. Bars represent means (n = 5). **f**, Stomatal aperture in humidity-treated leaves.
1145 The indicated plants were exposed to MH or HH for 1 h. Bars represent the median (n =
1146 220-247). **g**, Water-soaking in *Pst* Δ*hrcC*-inoculated leaves. The indicated plants were

1147 infiltrated with *Pst* Δ*hrcC* (OD_{600} = 0.02) and maintained under HH for 1 day. The number
1148 of water-soaked leaves was pooled from two independent experiments. **h**, **i**, Bacterial
1149 growth in *Pst* Δ*hrcC*-inoculated leaves. The indicated plants were infiltrated with *Pst*
1150 Δ*hrcC* (OD_{600} = 0.02) and maintained under HH (**h**) or MH (**i**) for 3 days. Bars represent
1151 means (n = 6). Different letters indicate statistically significant differences ($P < 0.05$; two-
1152 way ANOVA followed by Tukey's test in **b-f**; one-way ANOVA followed by Tukey's test
1153 in **h** and **i**). WT, wild-type; CAMTA3-A855V, a partial loss-of-function variant; dpi, days
1154 post-infiltration. Experiments in (**b-d**), (**f**), (**h**), and (**i**) were repeated twice with similar
1155 results.
1156

1157 **Fig. 5: *Pst* DC3000 blocks high humidity-driven plant transcriptome**
1158 **reprogramming via T3S effectors.**

1159 **a**, Schematic overview of the experimental design for analyzing high humidity-
1160 responsive gene expression in *Pst* DC3000-inoculated leaves. **b**, Bacterial titers in wild-
1161 type (WT) leaves infiltrated with *Pst* DC3000 or *Pst* Δ*hrcC* (OD_{600} = 0.02) at 8 hours
1162 post-infiltration (hpi) under moderate humidity (MH). Bars represent means (n = 6). **c**,
1163 Expression levels of *CYP707A3*, *CYP707A1*, and *NCED3* in *Pst* DC3000-inoculated
1164 leaves following humidity treatment. WT plants were infiltrated with the indicated *Pst*
1165 DC3000 strains (OD_{600} = 0.02), maintained under MH for 8 h, and then exposed to MH
1166 or high humidity (HH) for 0.5 h. Bars represent means (n = 3). **d**, **e**, Transcriptome
1167 profiling of *Pst* DC3000-inoculated leaves following humidity treatment as described in
1168 (**a**) and (**c**). **d**, Principal component analysis (PCA) of transcriptomic data. **e**, K-means-
1169 clustering of the 2000 most variable genes. Different letters indicate statistically
1170 significant differences ($P < 0.05$; Welch's t-test in **b**; two-way ANOVA followed by
1171 Tukey's test in **c**). Experiments in (**b**) and (**c**) were repeated twice with similar results.
1172

1173 **Fig. 6: T3S effector AvrPtoB suppresses *CYP707A3*-mediated water-soaking**
1174 **resistance.**

1175 **a**, Expression levels of *CYP707A3* in *Pst* DC3000-inoculated leaves following humidity
1176 treatment. Wild-type (WT) plants were infiltrated with the indicated *Pst* DC3000 strains
1177 (OD_{600} = 0.02), maintained under moderate humidity (MH) for 8 h, and then exposed to
1178 MH or high humidity (HH) for 0.5 h. Bars represent means (n = 3). The box highlights

1179 the effectors retained in *Pst* Δ20E but absent in *Pst* Δ28E. **b-d**, Expression levels of
1180 *CYP707A3* in humidity-treated leaves with or without induction of *AvrPtoB* (**b**), *AvrPto*
1181 (**c**), or *AvrPtoB-F479A* (**d**). The indicated plants were infiltrated with 0.1% ethanol
1182 (−DEX) or 10 μM DEX (+DEX), maintained under moderate humidity (MH) for 24 h,
1183 then exposed to MH or HH for 0.5 h. Bars represent means (n = 3). **e**, ABA levels in
1184 humidity-treated leaves with or without *AvrPtoB* induction. The indicated plants were
1185 treated with DEX as described in (**b-d**), and then exposed to MH or HH for 2 h. Bars
1186 represent means (n = 3). **f**, Stomatal aperture in humidity-treated leaves with or without
1187 *AvrPtoB* induction. The indicated were treated with DEX as described in (**b-d**), and then
1188 exposed to MH or HH for 1 h. Bars represent the median (n = 253-367). **g**, Water-soaking
1189 in *Pst* Δ*hrcC*-inoculated leaves with or without *AvrPtoB* induction. The indicated plants
1190 were infiltrated with *Pst* Δ*hrcC* (OD_{600} = 0.02) supplemented with −DEX or +DEX and
1191 maintained under HH for 1 day. The number of water-soaked leaves was pooled from two
1192 independent experiments. Different letters indicate statistically significant differences (P
1193 < 0.05; two-way ANOVA followed by Tukey's test). AvrPtoB-F479A, E3 ligase deficient
1194 variant; ND, not detected. Experiments in (**a-d**) and (**f**) were repeated twice with similar
1195 results.
1196
1197 **Fig. 7: *Pst* DC3000 employs AvrPtoB to suppress *CYP707A3* expression and promote**
1198 **water-soaking under high humidity.**
1199 **a**, Schematic overview of the experimental design for analyzing gene expression, ABA
1200 accumulation, water-soaking, and bacterial growth in *Pst* DC3000-inoculated leaves. **b**,
1201 Expression levels of *CYP707A3*, *CYP707A1*, and *NCED3* in *Pst* DC3000-inoculated
1202 leaves at 6 hours post-infiltration (hpi) under HH. Wild-type (WT) plants were infiltrated
1203 with the indicated *Pst* DC3000 strains (OD_{600} = 0.2), maintained under moderate humidity
1204 (MH) for 2 h, and then transferred to HH for 4 h. Bars represent means (n = 3). **c**, ABA
1205 levels in *Pst* DC3000-inoculated leaves. WT plants were inoculated with the indicated
1206 *Pst* DC3000 strains as described in (**b**). Bars represent means (n = 6). **d**, **e**, Representative
1207 images (**d**) and quantification (**e**) of water-soaking in *Pst* DC3000-inoculated leaves. WT
1208 and *cyp707a1 cyp707a3* mutant plants were infiltrated with the indicated *Pst* DC3000
1209 strains (OD_{600} = 0.2), maintained under MH for 2 h, and then transferred to HH for 20-22
1210 h. Bars represent the median (n = 36; pooled from two independent experiments). **f**, **g**,

1211 Disease symptoms (**f**) and bacterial growth (**g**) in *Pst* DC3000-inoculated leaves. WT and
1212 *cyp707a1 cyp707a3* mutant plants were infiltrated with the indicated *Pst* DC3000 strains
1213 (OD_{600} = 0.0002), maintained under MH for 2 h, and then transferred to HH for 3 days.
1214 Bars represent means (n = 6). Different letters indicate statistically significant differences
1215 (P < 0.05; one-way ANOVA followed by Tukey's test in **b** and **c**; two-way ANOVA
1216 followed by Tukey's test in **e** and **g**). dpi, days post-infiltration. Experiments in (**b**), (**f**),
1217 and (**g**) were repeated twice with similar results. **g**, Working model of *CYP707A3*-
1218 mediated water-soaking resistance and its suppression by *Pst* DC3000 via T3S effector
1219 AvrPtoB under high humidity.

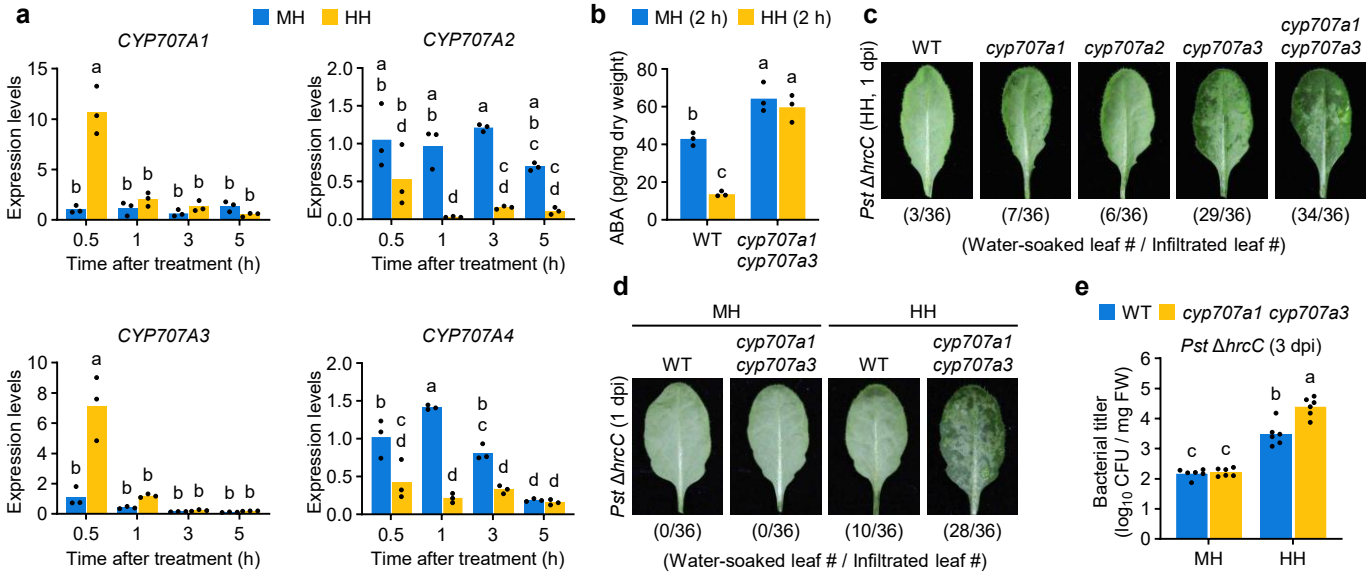

Fig. 1: *CYP707A3* is required for resistance to bacterial water-soaking under high humidity.
a, Expression levels of *CYP707A* genes in humidity-treated leaves. Wild-type (WT) plants were exposed to moderate humidity (MH) or high humidity (HH) for the indicated time. Bars represent means (n = 3). **b**, ABA levels in humidity-treated leaves. The indicated plants were exposed to MH or HH for 2 h. Bars represent means (n = 3). **c**, **d**, Water-soaking in *Pst* Δ*hrcC*-inoculated leaves. The indicated plants were infiltrated with *Pst* Δ*hrcC* (OD_{600} = 0.02) and maintained under MH or HH for 1 day. The number of water-soaked leaves was pooled from two independent experiments. **e**, Bacterial growth in *Pst* Δ*hrcC*-inoculated leaves. The indicated plants were infiltrated with *Pst* Δ*hrcC* (OD_{600} = 0.02) and maintained under MH or HH for 3 days. Bars represent means (n = 6). Different letters indicate statistically significant differences (P < 0.05; two-way ANOVA followed by Tukey's test). dpi, days post-infiltration. Experiments in (**a**) and (**e**) were repeated twice with similar results.

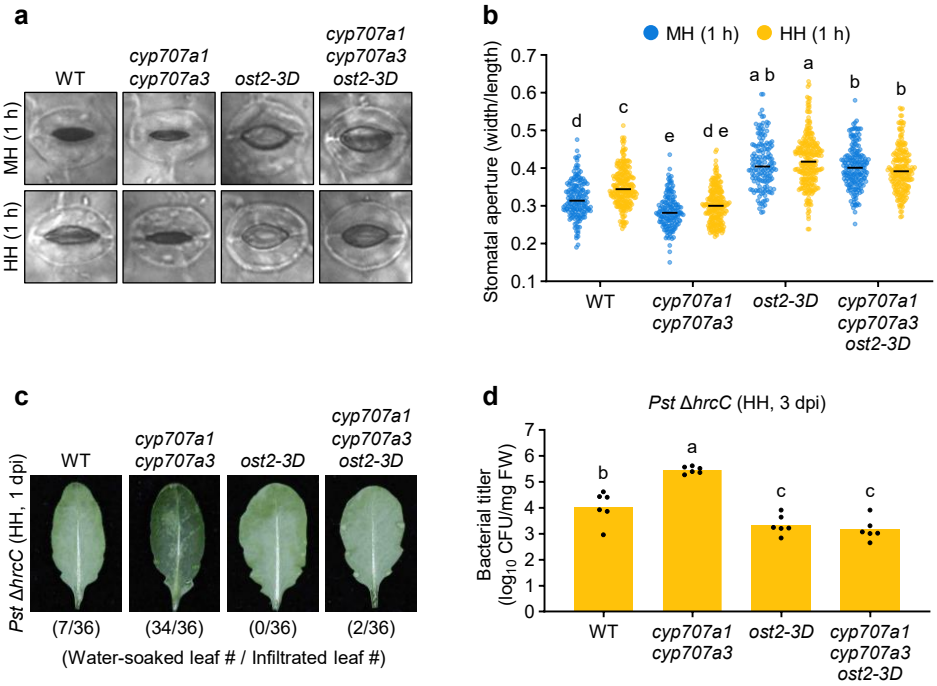

Fig. 2: *CYP707A3*-mediated water-soaking resistance depends on stomatal opening.
a, **b**, Representative images of stomata (**a**) and stomatal aperture (**b**) in humidity-treated leaves. The indicated plants were exposed to moderate humidity (MH) or high humidity (HH) for 1 h. Bars represent the median (n = 149-264). **c**, Water-soaking in *Pst* Δ*hrcC*-inoculated leaves. The indicated plants were infiltrated with *Pst* Δ*hrcC* (OD_{600} = 0.02) and maintained under HH for 1 day. The number of water-soaked leaves was pooled from two independent experiments. **d**, Bacterial growth in *Pst* Δ*hrcC*-inoculated leaves. The indicated plants were infiltrated with *Pst* Δ*hrcC* (OD_{600} = 0.02) and maintained under HH for 3 days. Bars represent means (n = 6). Different letters indicate statistically significant differences ($P < 0.05$; two-way ANOVA followed by Tukey's test in **b**; one-way ANOVA followed by Tukey's test in **d**). WT, wild-type; dpi, days post-infiltration. Experiments in (**b**) and (**d**) were repeated twice with similar results.

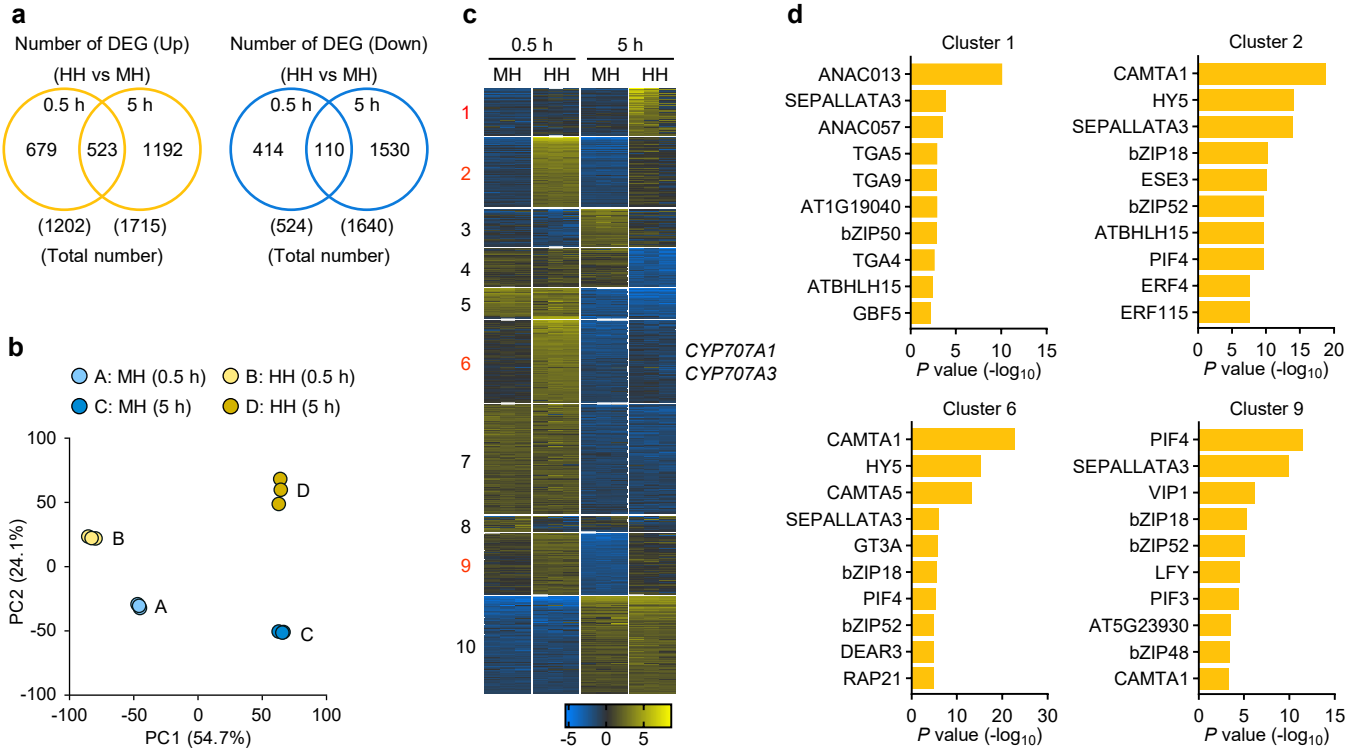

Fig. 3: CAMTA binding motifs are overrepresented in early-phase high humidity-induced genes. **a-c**, Transcriptome profiling of humidity-treated leaves by RNA-seq. Wild-type plants were exposed to moderate humidity (MH) or high humidity (HH) for the indicated time. **a**, Venn diagrams showing differentially expressed genes (DEGs) (fold change > 2; FDR < 0.05) at 0.5 h and 5 h after treatment. **b**, Principal component analysis (PCA) of transcriptomic data. **c**, K-means clustering of the 1000 most variable genes. **d**, Top 10 enriched *cis*-regulatory elements among high humidity-induced genes identified in the clusters shown in (**c**).

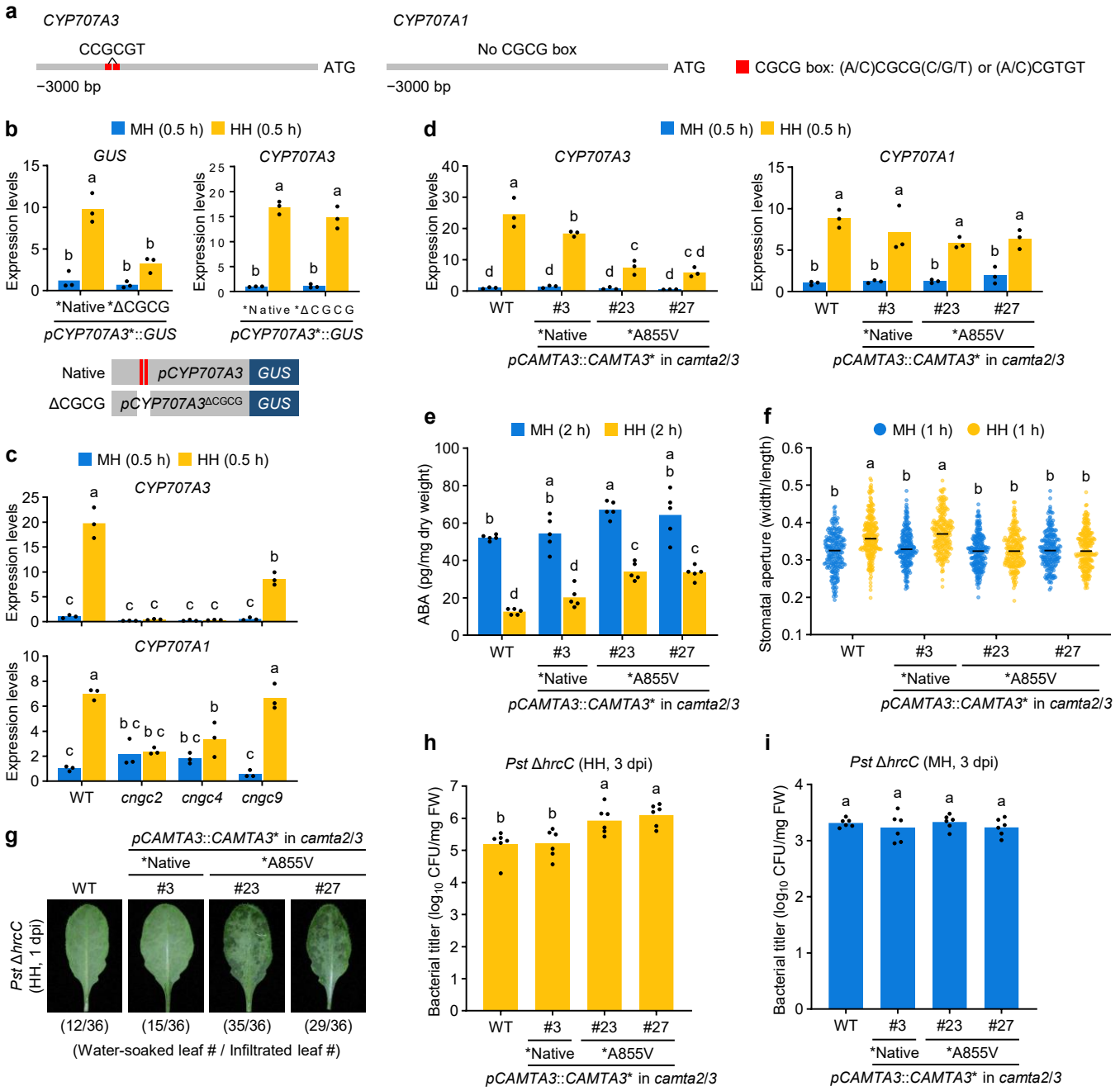

Fig. 4: CAMTA3 drives *CYP707A3* expression to promote resistance to bacterial water-soaking under high humidity.

a, Schematic diagram of the promoter regions of *CYP707A3* and *CYP707A1*, highlighting the CGCG box. **b**, *GUS* expression driven by the *CYP707A3* promoter, with or without CGCG boxes, in humidity-treated leaves. The indicated constructs were transiently expressed in *NahG* leaves via *Agrobacterium* infiltration. Infiltrated plants were maintained under moderate humidity (MH) for 24 h, then exposed to MH or high humidity (HH) for 0.5 h. Bars represent means (n = 3). **c**, **d**, Expression levels of *CYP707A3* and *CYP707A1* in humidity-treated leaves of *cngc* (**c**) and *camta3* (**d**) mutants. The indicated plants were exposed to MH or HH for 0.5 h. Bars represent means (n = 3). **e**, ABA levels in humidity-treated leaves. The indicated plants were exposed to MH or HH for 2 h. Bars represent means (n = 5). **f**, Stomatal aperture in humidity-treated leaves. The indicated plants were exposed to MH or HH for 1 h. Bars represent the median (n = 220-247). **g**, Water-soaking in *Pst ΔhrcC*-inoculated leaves. The indicated plants were infiltrated with *Pst ΔhrcC* (OD_{600} = 0.02) and maintained under HH for 1 day. The number of water-soaked leaves was pooled from two independent experiments. **h**, **i**, Bacterial growth in *Pst ΔhrcC*-inoculated leaves. The indicated plants were infiltrated with *Pst ΔhrcC* (OD_{600} = 0.02) and maintained under HH (**h**) or MH (**i**) for 3 days. Bars represent means (n = 6). Different letters indicate statistically significant differences (P < 0.05; two-way ANOVA followed by Tukey's test in **b-f**; one-way ANOVA followed by Tukey's test in **h** and **i**). WT, wild-type; CAMTA3-A855V, a partial loss-of-function variant; dpi, days post-infiltration. Experiments in (**b-d**), (**f**), (**h**), and (**i**) were repeated twice with similar results.

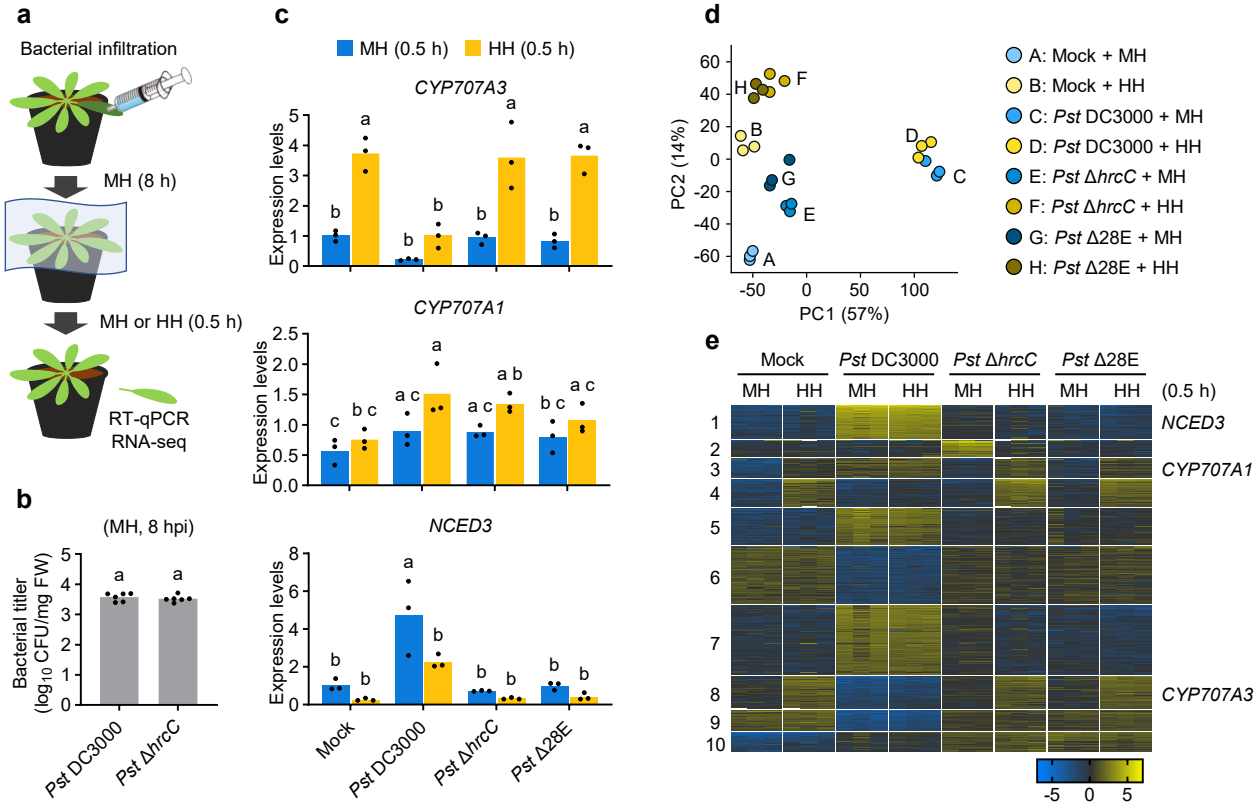

Fig. 5: *Pst* DC3000 blocks high humidity-driven plant transcriptome reprogramming via T3S effectors.

a, Schematic overview of the experimental design for analyzing high humidity-responsive gene expression in *Pst* DC3000-inoculated leaves. **b**, Bacterial titers in wild-type (WT) leaves infiltrated with *Pst* DC3000 or *Pst* Δ*hrcC* (OD_{600} = 0.02) at 8 hours post-infiltration (hpi) under moderate humidity (MH). Bars represent means (n = 6). **c**, Expression levels of *CYP707A3*, *CYP707A1*, and *NCED3* in *Pst* DC3000-inoculated leaves following humidity treatment. WT plants were infiltrated with the indicated *Pst* DC3000 strains (OD_{600} = 0.02), maintained under MH for 8 h, and then exposed to MH or high humidity (HH) for 0.5 h. Bars represent means (n = 3). **d**, **e**, Transcriptome profiling of *Pst* DC3000-inoculated leaves following humidity treatment as described in (**a**) and (**c**). **d**, Principal component analysis (PCA) of transcriptomic data. **e**, K-means-clustering of the 2000 most variable genes. Different letters indicate statistically significant differences (P < 0.05; Welch's t-test in **b**; two-way ANOVA followed by Tukey's test in **c**). Experiments in (**b**) and (**c**) were repeated twice with similar results.

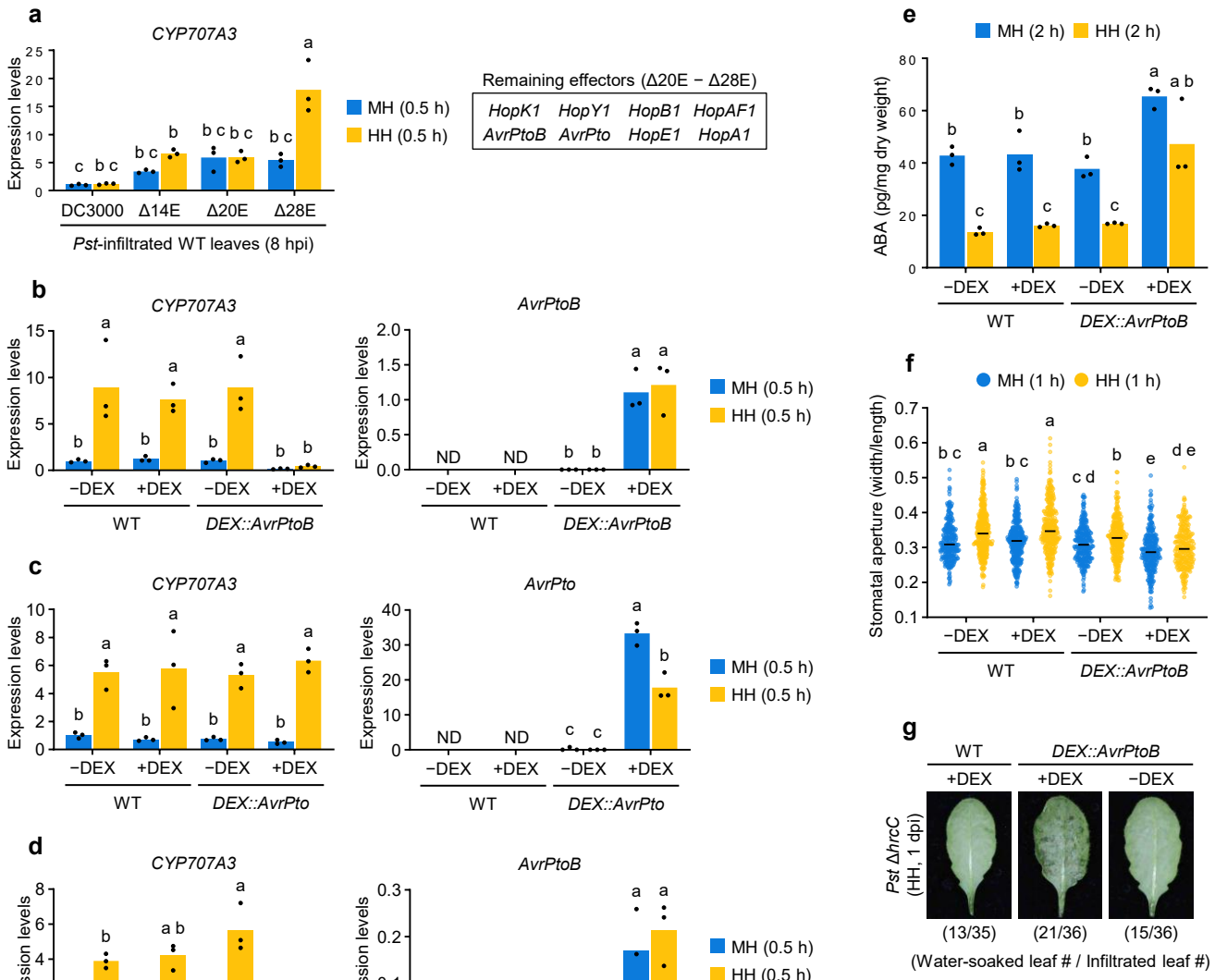

Fig. 6: T3S effector AvrPtoB suppresses *CYP707A3*-mediated water-soaking resistance.
a, Expression levels of *CYP707A3* in *Pst* DC3000-inoculated leaves following humidity treatment. Wild-type (WT) plants were infiltrated with the indicated *Pst* DC3000 strains (OD_{600} = 0.02), maintained under moderate humidity (MH) for 8 h, and then exposed to MH or high humidity (HH) for 0.5 h. Bars represent means (n = 3). The box highlights the effectors retained in *Pst* Δ20E but absent in *Pst* Δ28E. **b-d**, Expression levels of *CYP707A3* in humidity-treated leaves with or without induction of *AvrPtoB* (**b**), *AvrPto* (**c**), or *AvrPtoB-F479A* (**d**). The indicated plants were infiltrated with 0.1% ethanol (−DEX) or 10 μM DEX (+DEX), maintained under moderate humidity (MH) for 24 h, then exposed to MH or HH for 0.5 h. Bars represent means (n = 3). **e**, ABA levels in humidity-treated leaves with or without *AvrPtoB* induction. The indicated plants were treated with DEX as described in (**b-d**), and then exposed to MH or HH for 2 h. Bars represent means (n = 3). **f**, Stomatal aperture in humidity-treated leaves with or without *AvrPtoB* induction. The indicated were treated with DEX as described in (**b-d**), and then exposed to MH or HH for 1 h. Bars represent the median (n = 253-367). **g**, Water-soaking in *Pst* Δ*hrcC*-inoculated leaves with or without *AvrPtoB* induction. The indicated plants were infiltrated with *Pst* Δ*hrcC* (OD_{600} = 0.02) supplemented with −DEX or +DEX and maintained under HH for 1 day. The number of water-soaked leaves was pooled from two independent experiments. Different letters indicate statistically significant differences (P < 0.05; two-way ANOVA followed by Tukey's test). AvrPtoB-F479A, E3 ligase deficient variant; ND, not detected. Experiments in (**a-d**) and (**f**) were repeated twice with similar results.

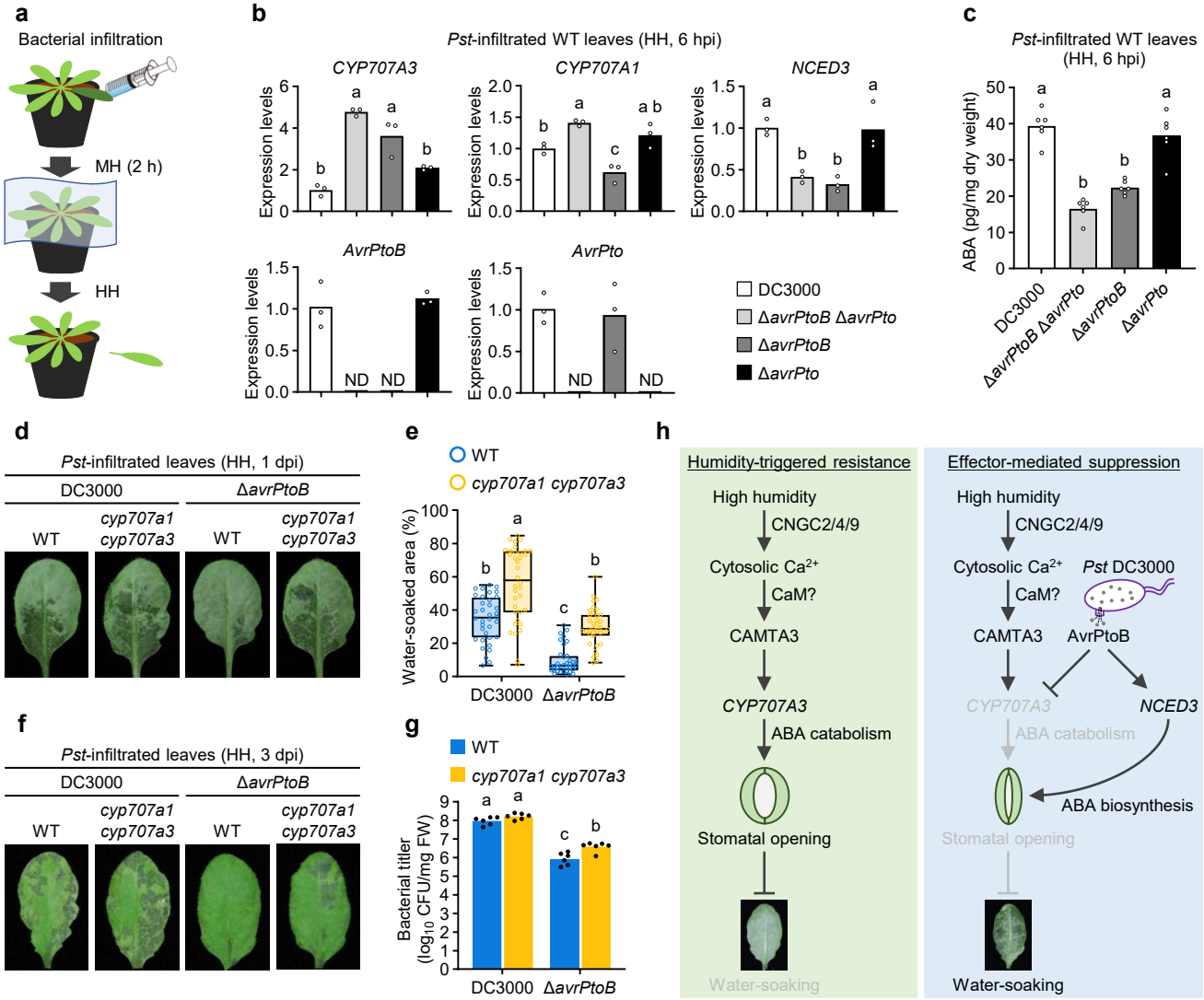

Fig. 7: *Pst* DC3000 employs AvrPtoB to suppress *CYP707A3* expression and promote water-soaking under high humidity.

a, Schematic overview of the experimental design for analyzing gene expression, ABA accumulation, water-soaking, and bacterial growth in *Pst* DC3000-inoculated leaves. **b**, Expression levels of *CYP707A3*, *CYP707A1*, and *NCED3* in *Pst* DC3000-inoculated leaves at 6 hours post-infiltration (hpi) under HH. Wild-type (WT) plants were infiltrated with the indicated *Pst* DC3000 strains (OD_{600} = 0.2), maintained under moderate humidity (MH) for 2 h, and then transferred to HH for 4 h. Bars represent means (n = 3). **c**, ABA levels in *Pst* DC3000-inoculated leaves. WT plants were inoculated with the indicated *Pst* DC3000 strains as described in (**b**). Bars represent means (n = 6). **d**, **e**, Representative images (**d**) and quantification (**e**) of water-soaking in *Pst* DC3000-inoculated leaves. WT and *cyp707a1 cyp707a3* mutant plants were infiltrated with the indicated *Pst* DC3000 strains (OD_{600} = 0.2), maintained under MH for 2 h, and then transferred to HH for 20-22 h. Bars represent the median (n = 36; pooled from two independent experiments). **f**, **g**, Disease symptoms (**f**) and bacterial growth (**g**) in *Pst* DC3000-inoculated leaves. WT and *cyp707a1 cyp707a3* mutant plants were infiltrated with the indicated *Pst* DC3000 strains (OD_{600} = 0.0002), maintained under MH for 2 h, and then transferred to HH for 3 days. Bars represent means (n = 6). Different letters indicate statistically significant differences ($P < 0.05$; one-way ANOVA followed by Tukey's test in **b** and **c**; two-way ANOVA followed by Tukey's test in **e** and **g**). dpi, days post-infiltration. Experiments in (**b**), (**f**), and (**g**) were repeated twice with similar results. **g**, Working model of *CYP707A3*-mediated water-soaking resistance and its suppression by *Pst* DC3000 via T3S effector AvrPtoB under high humidity.